PCA

- Principal Component Analysis
- 對一組高維度空間中的資料投影到低維度空間
- 找出最佳的投影方式，使得投影後的資料點能盡量散開

- 多光譜與高光譜

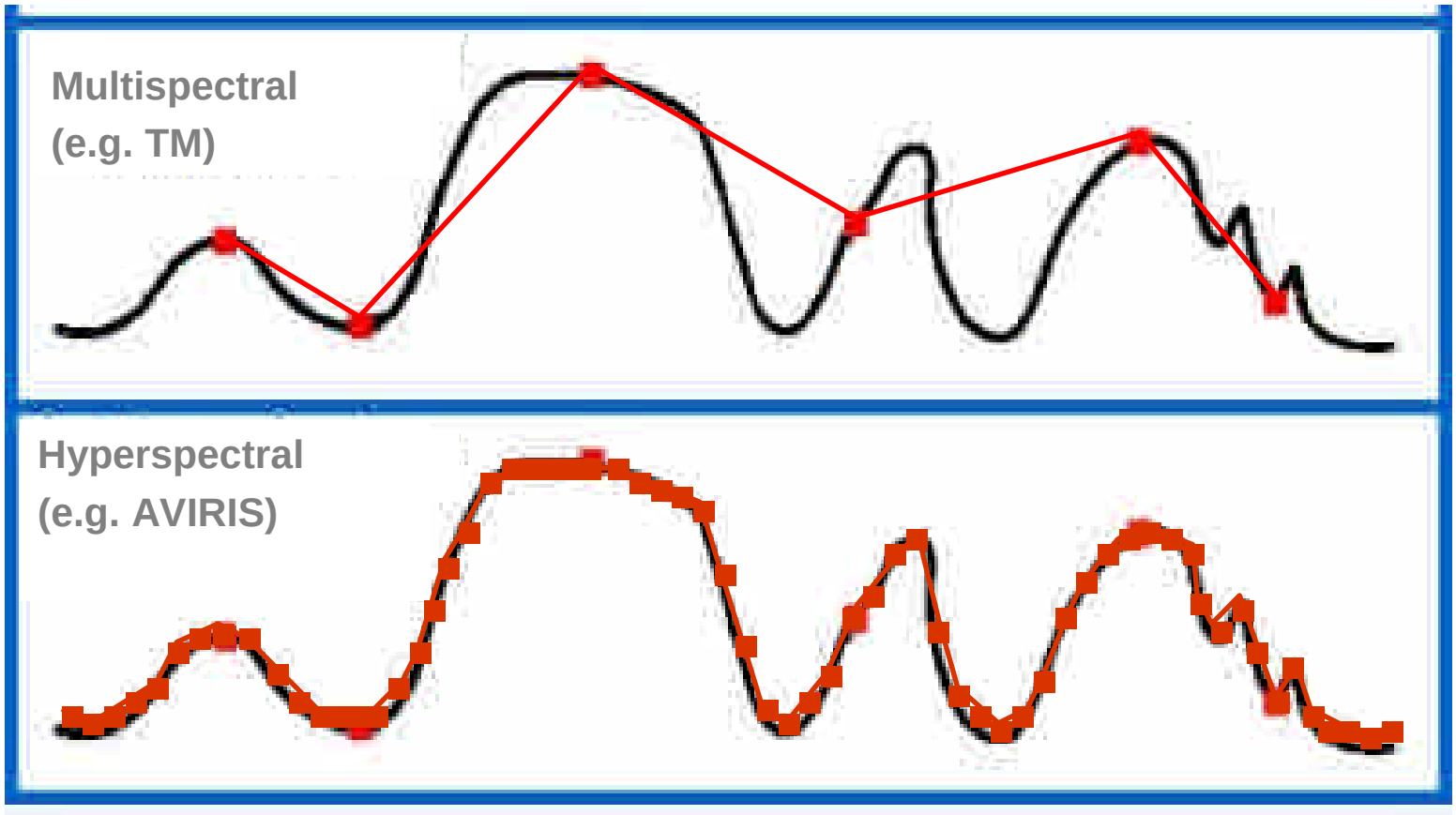

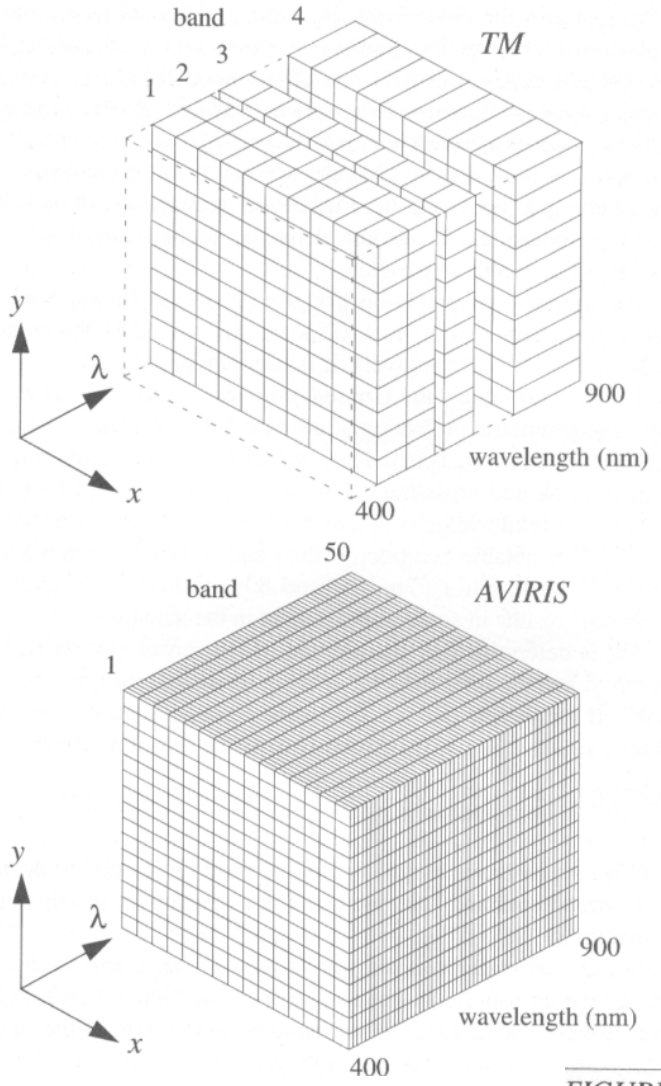

FIGURE 1-7. Visualization of the spatial and spectral resolutions of the Landsat TM and AVIRIS in the VNIR spectral range. The relative proportions between the two sensors are correct along each axis, and each small rectangular box represents one image pixel. The TM samples the spectral dimension incompletely and with relatively broad spectral bands. In comparison, AVIRIS represents almost a continuous spectral sampling. It also has a somewhat smaller GIFOV. This volume visualization is called an "image cube."

Example

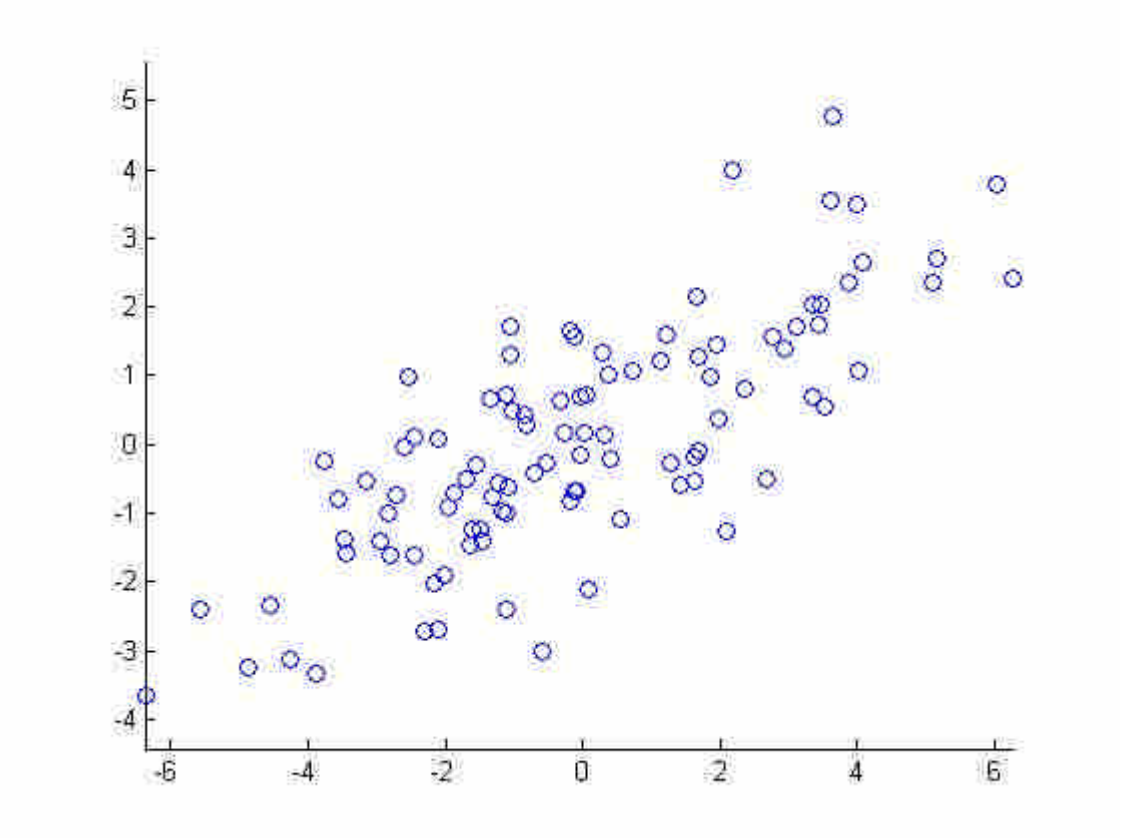

原始資料

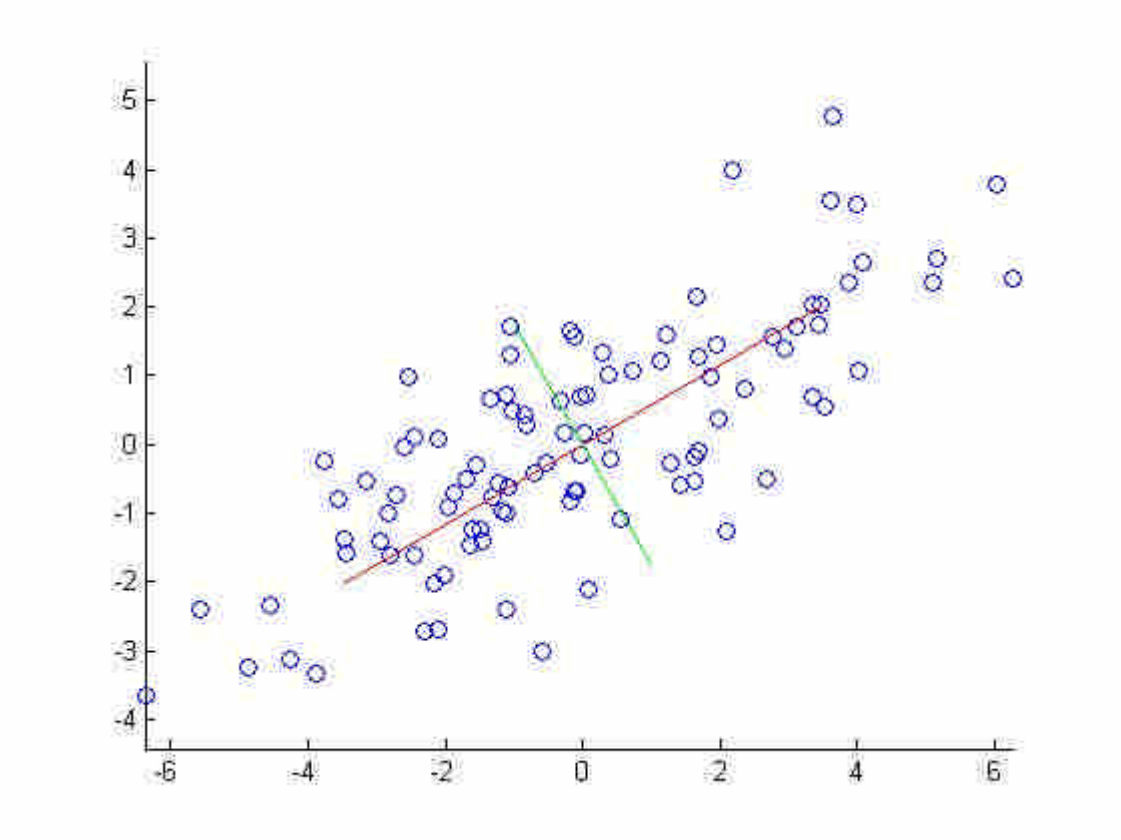

兩各主軸方向

假設我們的資料點是由維度爲m的向量Xi來表，其中 $i = 1,2,\ldots,n$

假設這一組資料的平均值是零：

$$\sum_{i=1}^{n} X_i = 0$$

目標是要找一個單位向量u，使得在u方向的投影平方和爲最大

用一個 $m \times n$ 矩陣A來表示此資料

$$A = \begin{bmatrix} X_1 & X_2 & X_3 & \cdots & X_n \end{bmatrix}$$

這一組資料在方向的投影可以表示爲下列向量：

$$p = \begin{bmatrix} X_1^T u \\ X_2^T u \\ \vdots \\ X_n^T u \end{bmatrix} = A^T u$$

投影平方的總和爲：

$$J(u) = \|p\|^2 = p^T p = \left(A^T u\right)^T \left(A^T u\right) = u^T A A^T u$$

欲使投影總和爲最大，並滿足 $\|u\|=1$，
我們可引進Lagrange Multiplier，並形
成新的目標函數：

$$\tilde{J}(u)=u^T AA^T u-\lambda\left(u^T u-1\right)$$

微分取極值 $\nabla_u \tilde{J}=0\Rightarrow 2AA^T u-2\lambda u=0$

$$\Rightarrow AA^T u=\lambda u$$

根據線性代數

λ爲AA^T的*eigenvalue*

u爲AA^T的*eigenvector*

AA^T eigenvalue的大小排列

$$\lambda_1 \geq \lambda_2 \geq \lambda_3 \geq \cdots \geq \lambda_m$$

對應的eigenvector則是

$$u_1, u_2, u_3 \cdots u_m$$

透過PCA，我們能找出一組單位向量 $\{ u_1, u_2, u_3 \cdots u_m \}$，使得

$$y_i = A^T u_i$$

其中，yi 稱爲第 i 組主要分量（the i-th principal component）。

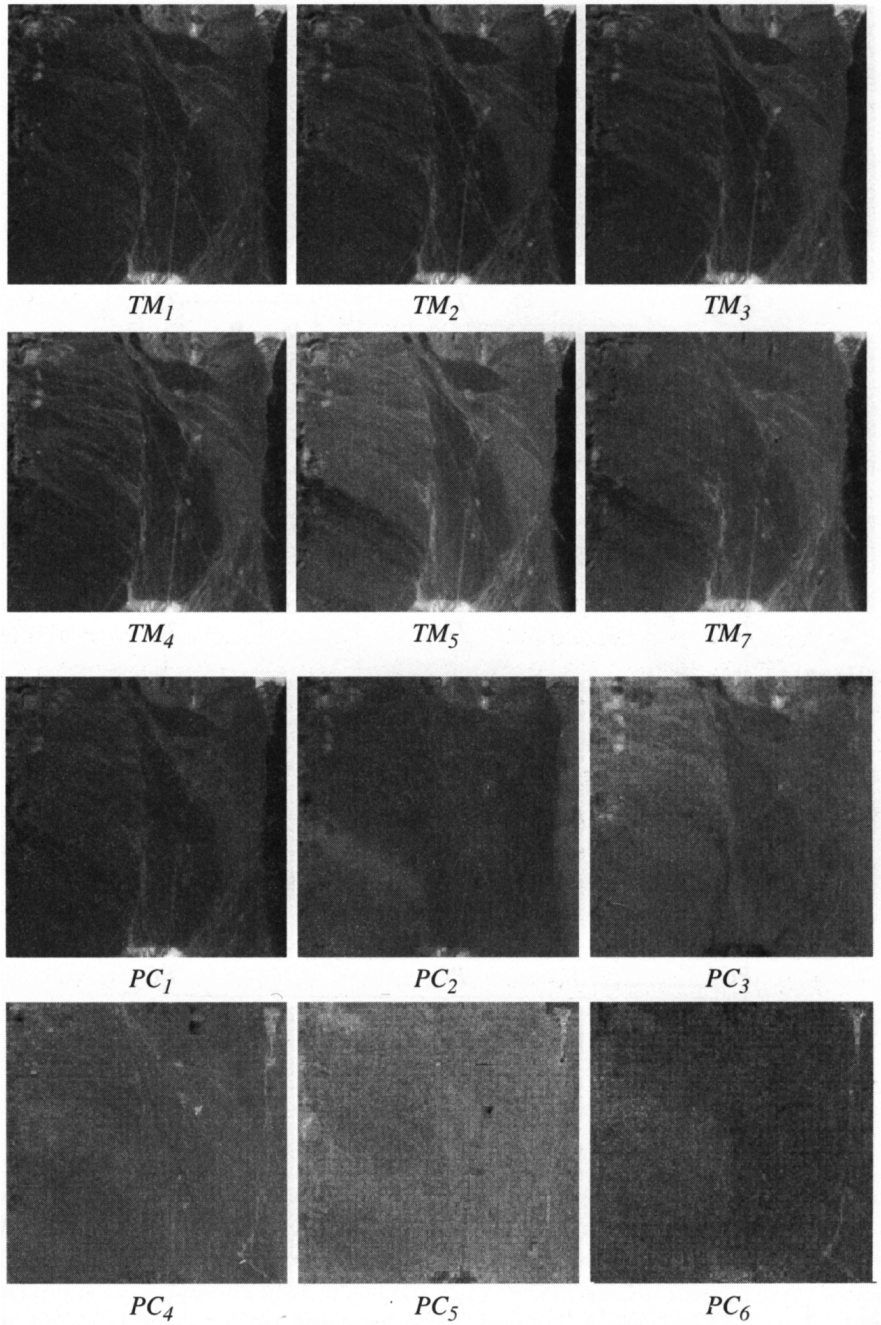

FIGURE 5-13. PC transformation of a nonvegetated TM scene.

Example

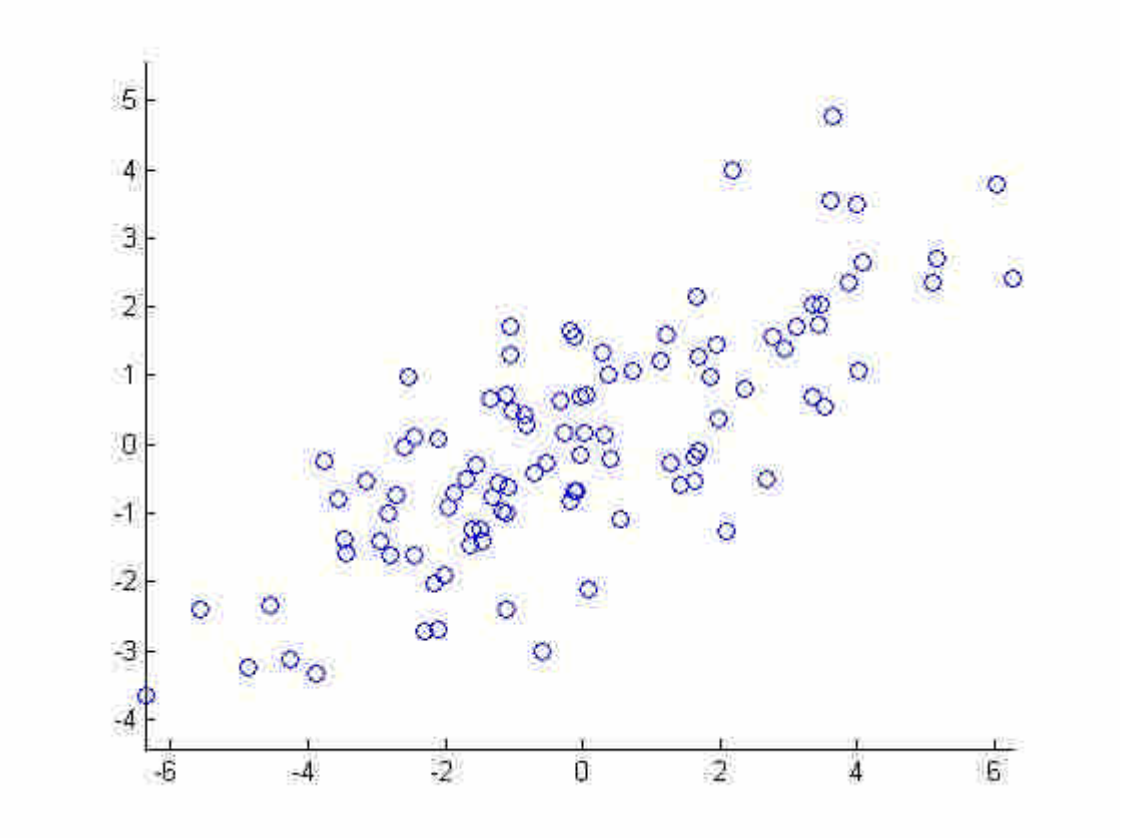

原始資料

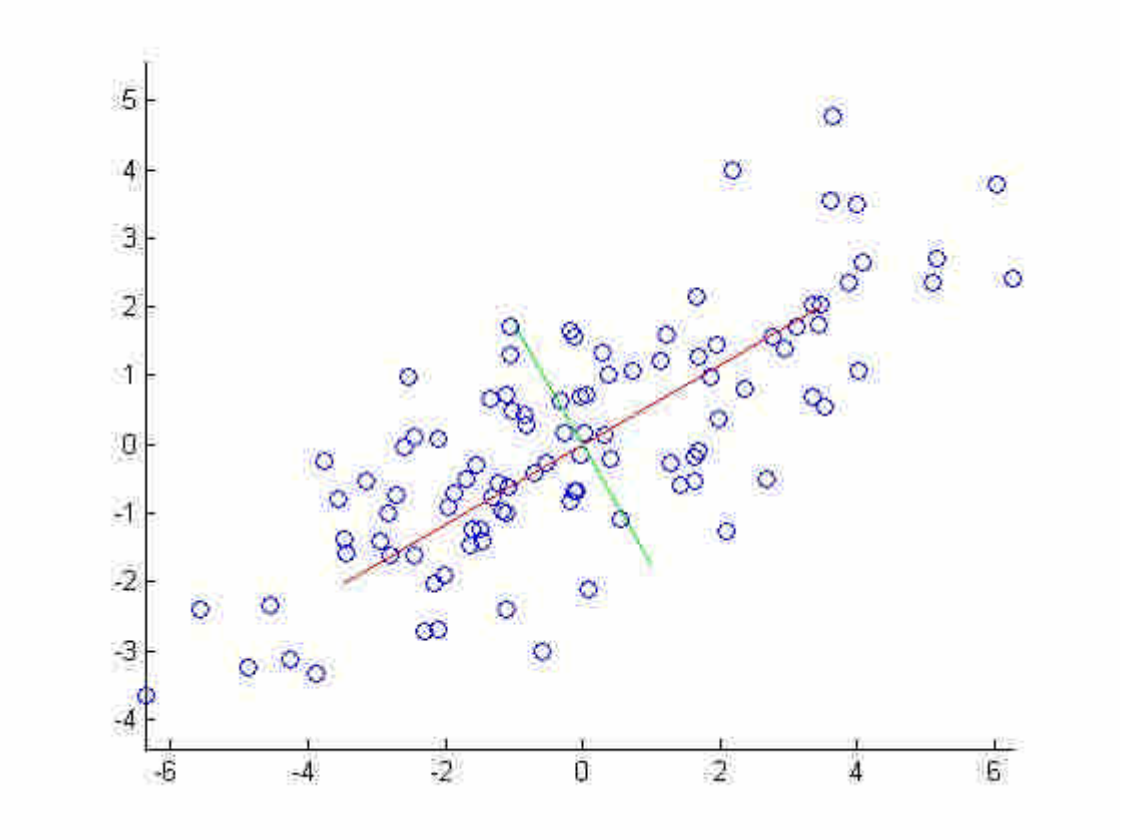

兩各主軸方向

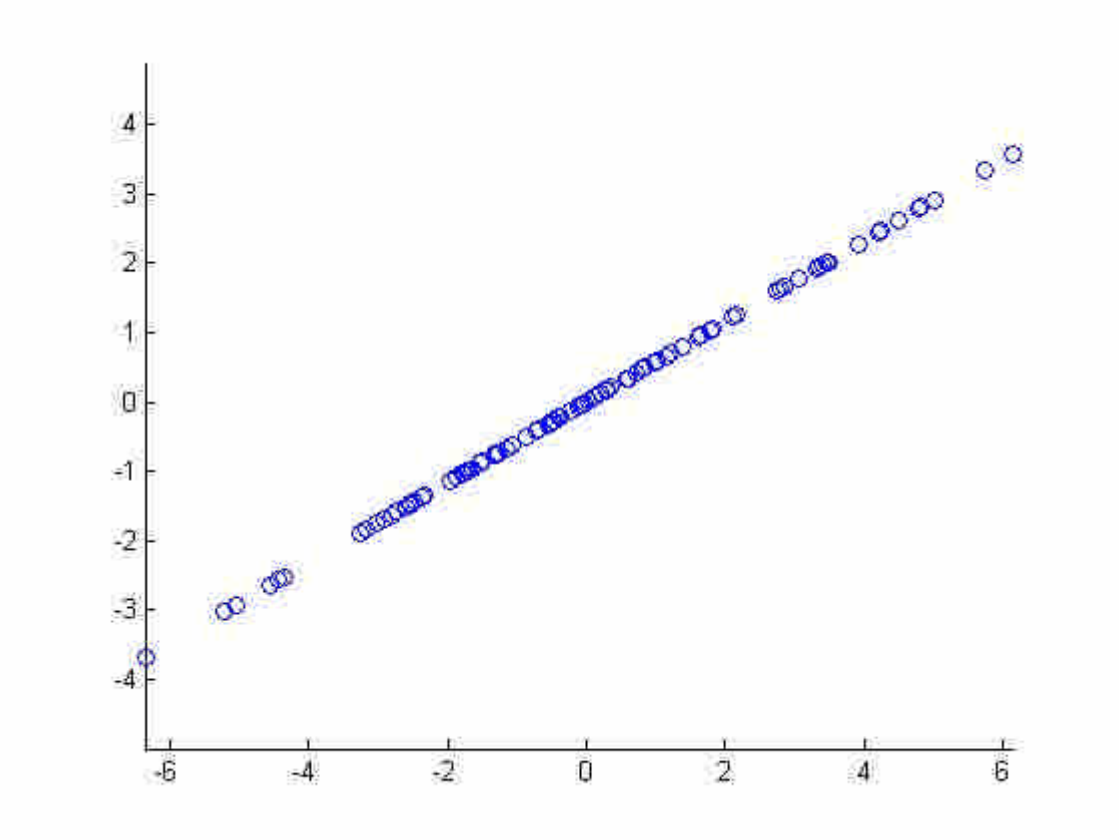

對**PC1**投影結果

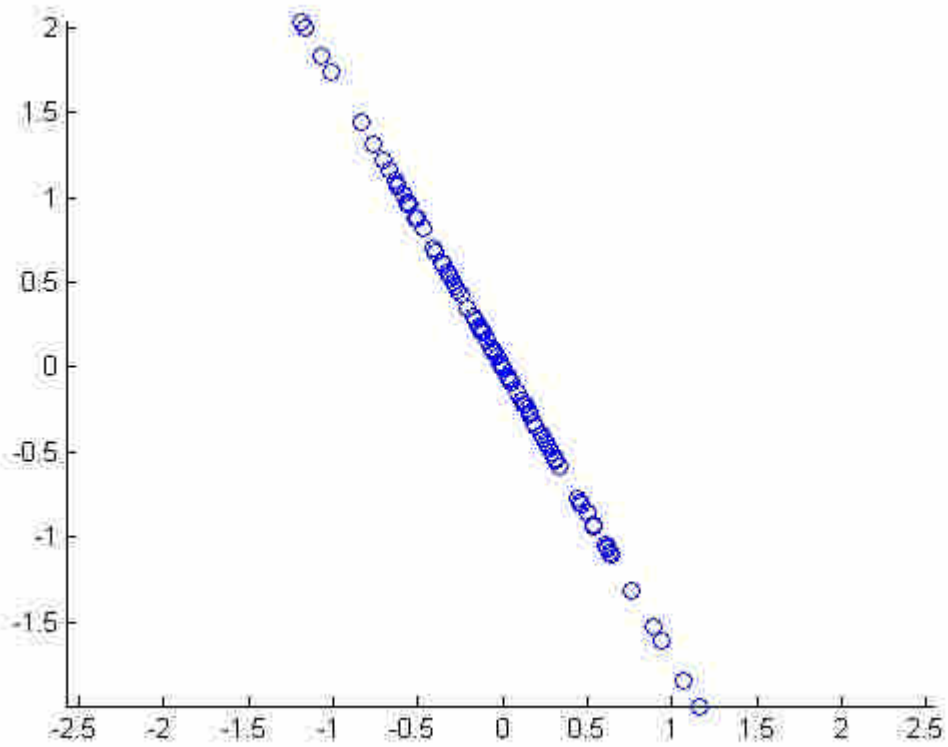

對**PC2**投影結果

Example

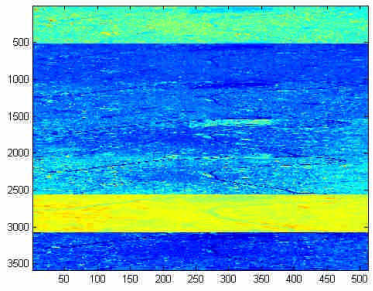

A

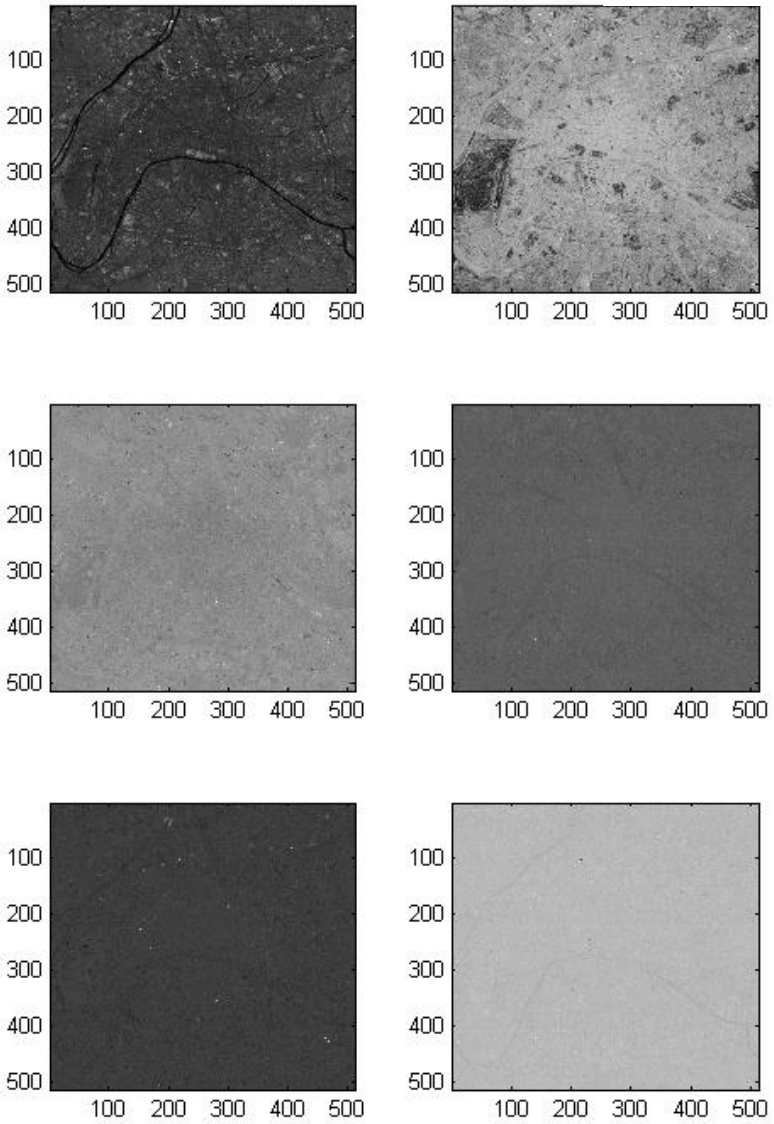

PCA

```
fid=fopen('paris.lan','r');
fseek(fid,128,-1);
A=fread(fid,[512*7,512],'uint8');
imagesc(A)
for i=1:7
A1(:,:,i)=A(512*(i-1)+1:512*i,:)';
end

A1(:,:,6)=[];
z=reshape(A1,512*512,6)';
R=(z-
repmat(mean(z')',1,512*512))*(z-
repmat(mean(z')',1,512*512))';
R=R/(512*512);
[V,D]=eig(R);
diag(D) PC=fliplr(V)'*z;
for i=1:6
subplot(3,2,i)
imagesc(reshape(PC(i,:),512,512
))
end
colormap(gray)
```

遙測影像特性

空間解析度

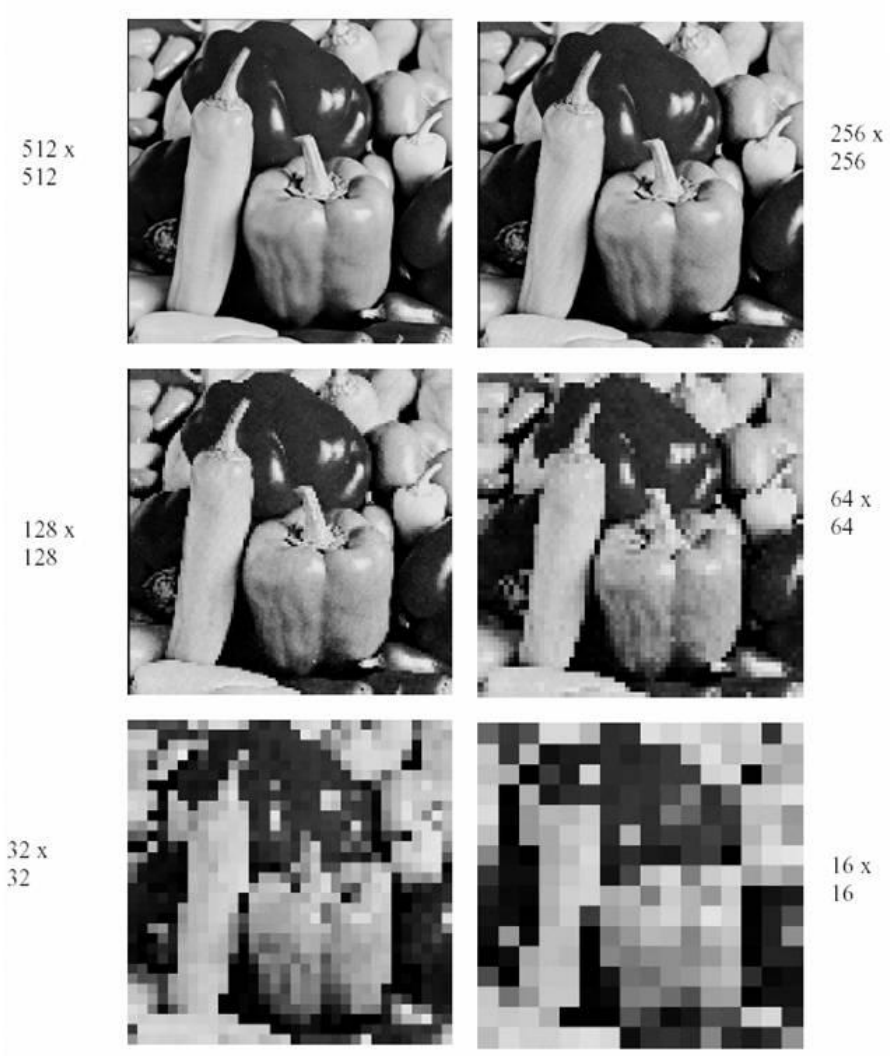

空間解析度

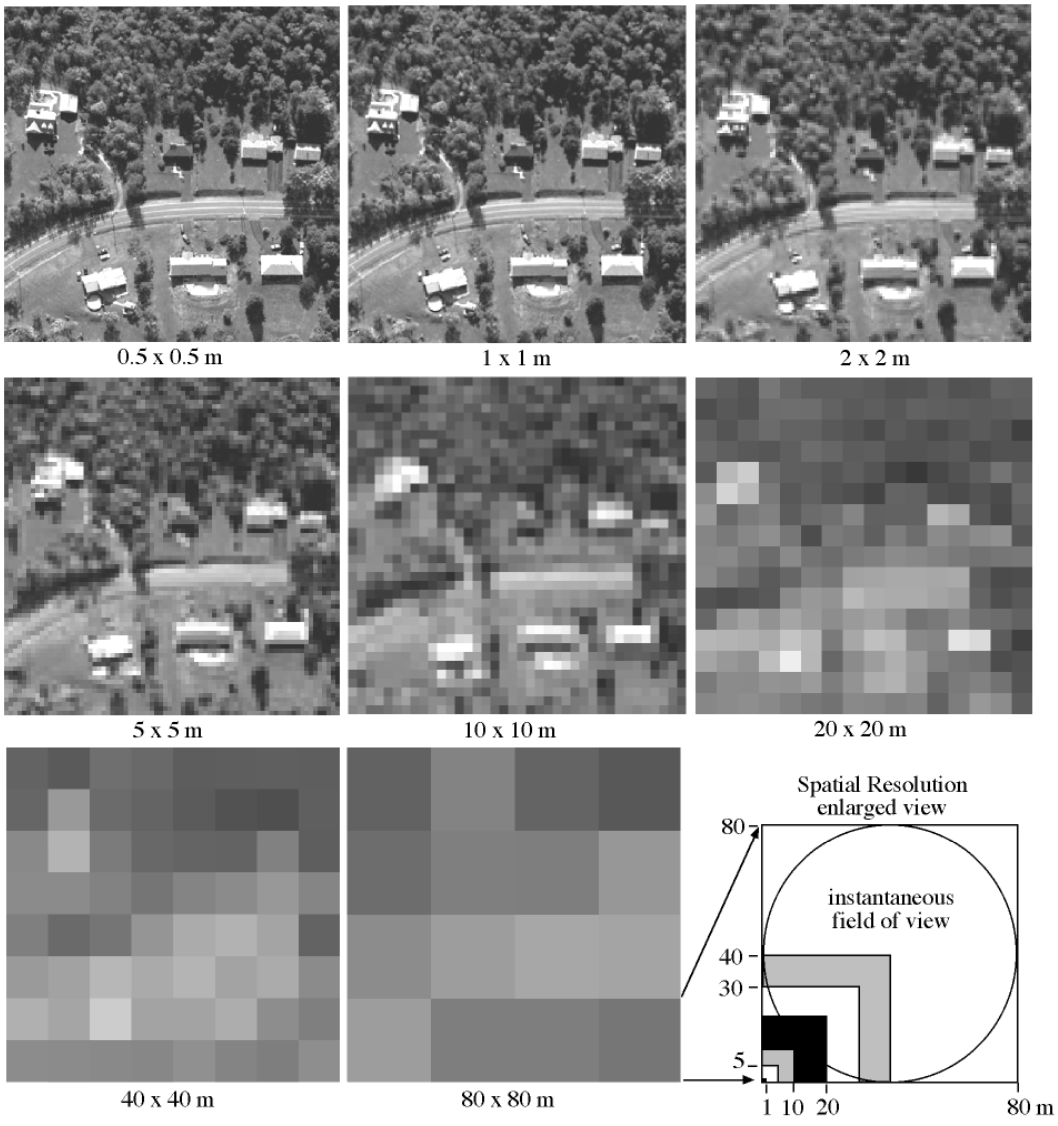
0.5 x 0.5 m
1 x 1 m
2 x 2 m
5 x 5 m
10 x 10 m
20 x 20 m
40 x 40 m
80 x 80 m
Spatial Resolution
enlarged view
80
instantaneous
field of view
40
30
5
1 10 20
80 m

- 影像壓縮
  - Box Pyramids
  - Gaussian Pyramids

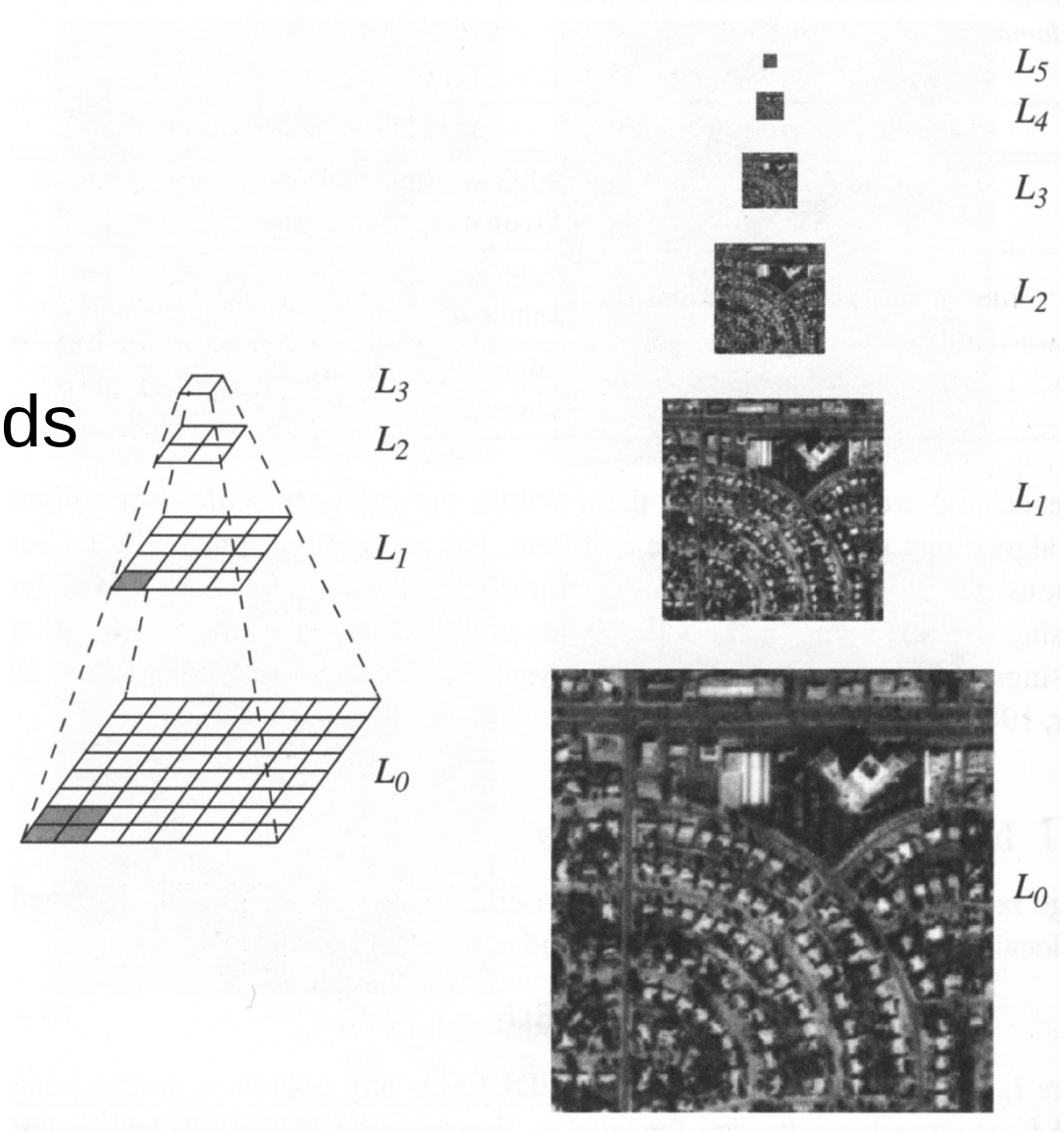

$$w_{mn} = \begin{bmatrix} 0.0025 & 0.0125 & 0.0200 & 0.0125 & 0.0025 \\ 0.0125 & 0.0625 & 0.1000 & 0.0625 & 0.0125 \\ 0.0200 & 0.1000 & 0.1600 & 0.1000 & 0.0200 \\ 0.0125 & 0.0625 & 0.1000 & 0.0625 & 0.0125 \\ 0.0025 & 0.0125 & 0.0200 & 0.0125 & 0.0025 \end{bmatrix} . \qquad (6-32)$$

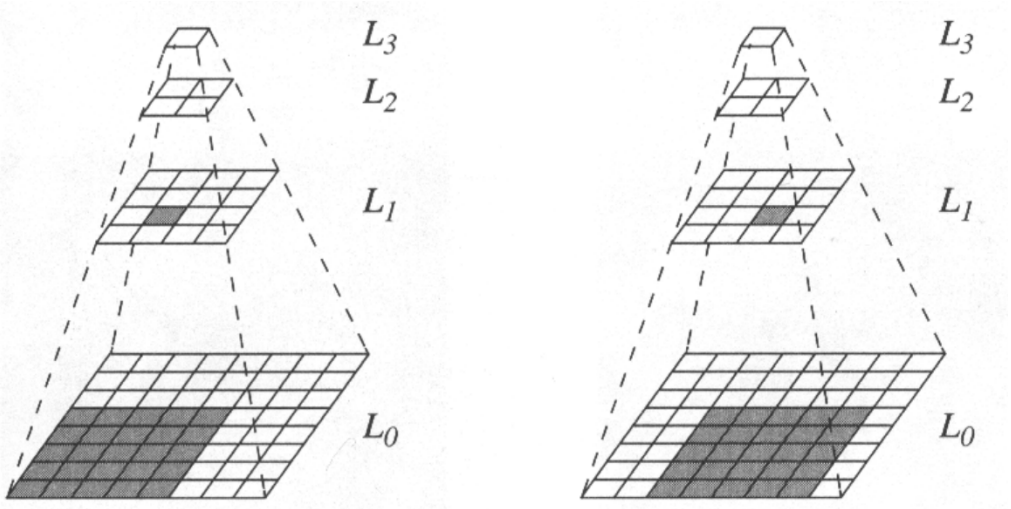

FIGURE 6-28. Gaussian pyramid construction with the 5 x 5 pixel weighting function of Eq. (6 – 32). On the left, the weighted average of 25 pixels in level 0 gives the shaded pixel in level 1. On the right, the weighting function is moved two pixels along a row and the weighted average of the corresponding pixels gives the next pixel in level 1. This process is repeated across the image in level 0, and then performed on level 1 to calculate level 2, and so forth. In this way, the linear size of the image is reduced by two from level to level. This is equivalent to a full convolution of level 0 with the weighting function, followed by a down-sample, but avoids unnecessary calculations. The border pixels require special attention as discussed earlier.

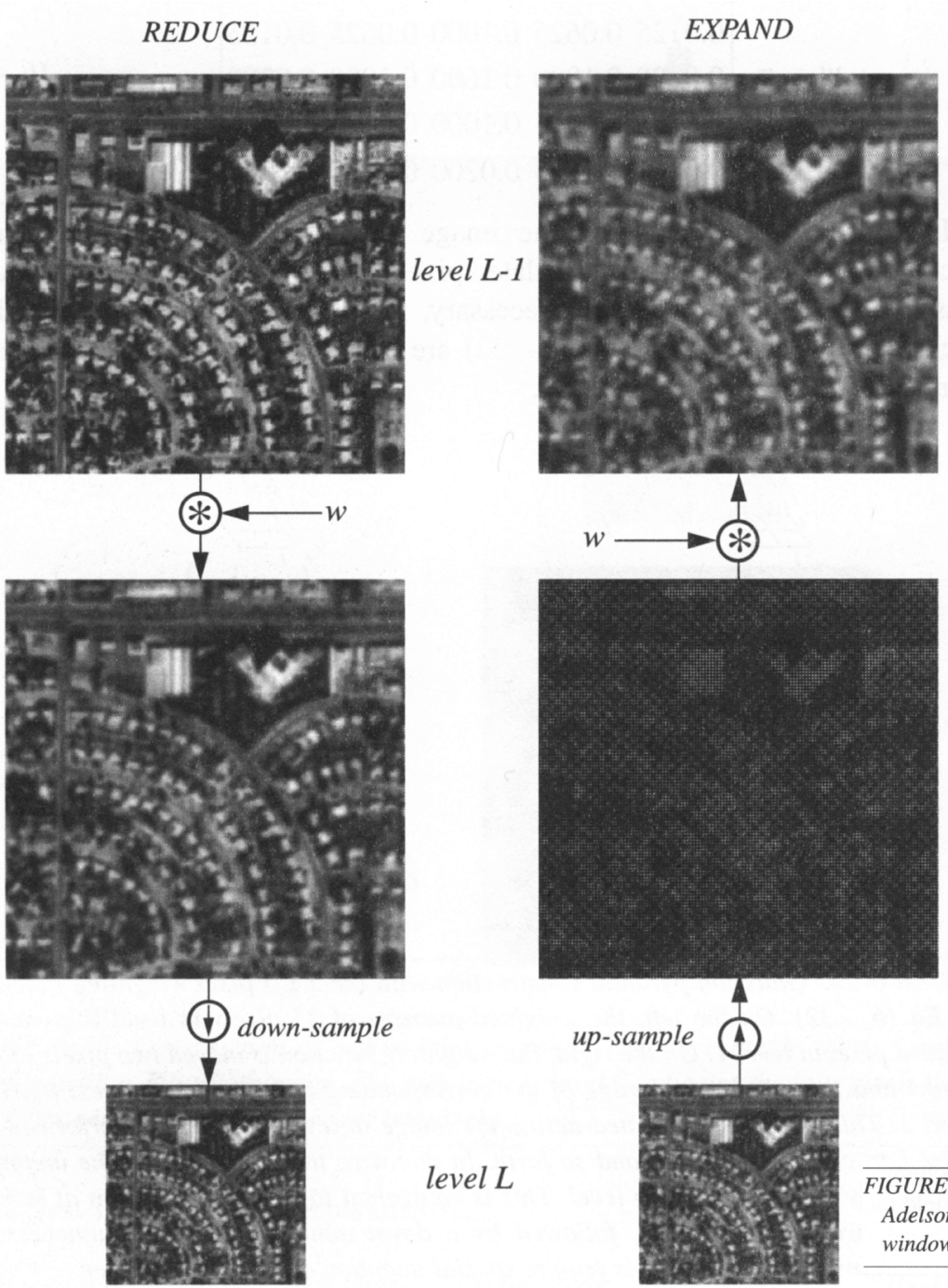

FIGURE 6-29. The REDUCE and EXPAND procedures as defined in (Burt and Adelson, 1983). Any spatial filter can be used, but these examples use the Gaussian window of Eq. (6 – 32).

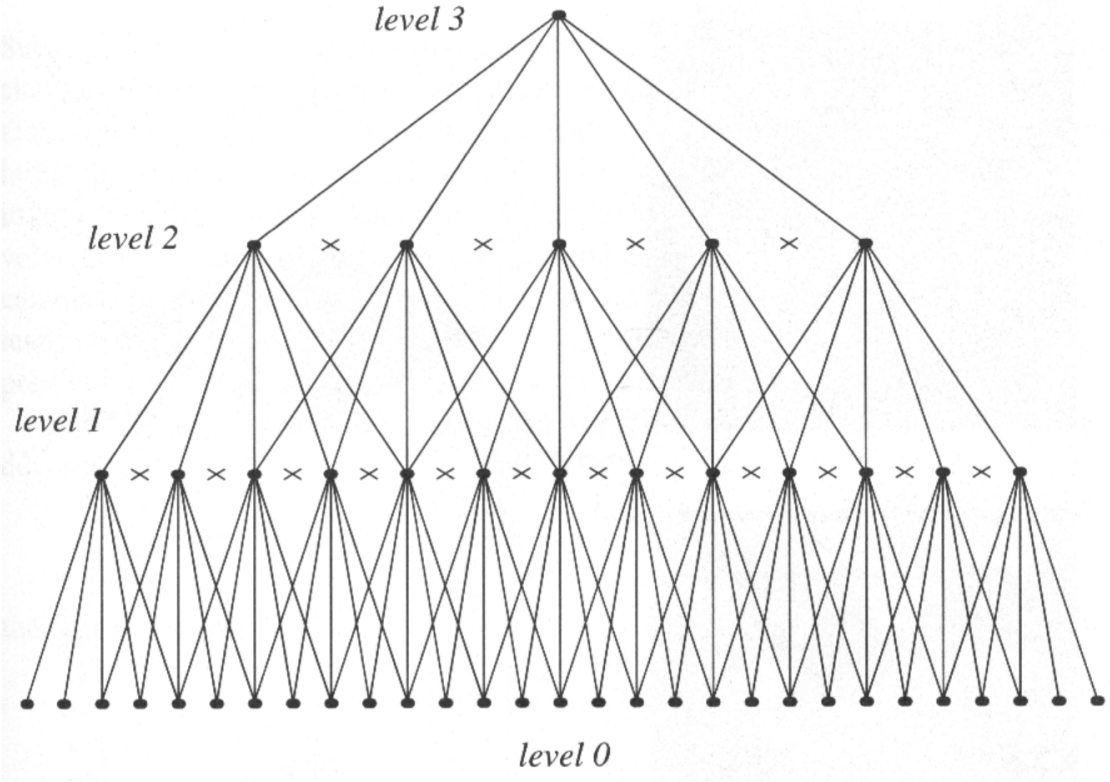

FIGURE 6-32. The links between a pixel in level 3 of the Gaussian pyramid and pixels at lower levels. The x-marks indicate pixels that are not included at each level because of downsampling. The effective convolution window size at the original level 0 for a pyramid that reduces by two at each level L is $4(2^L - 1) + 1$ *(Burt, 1981).*

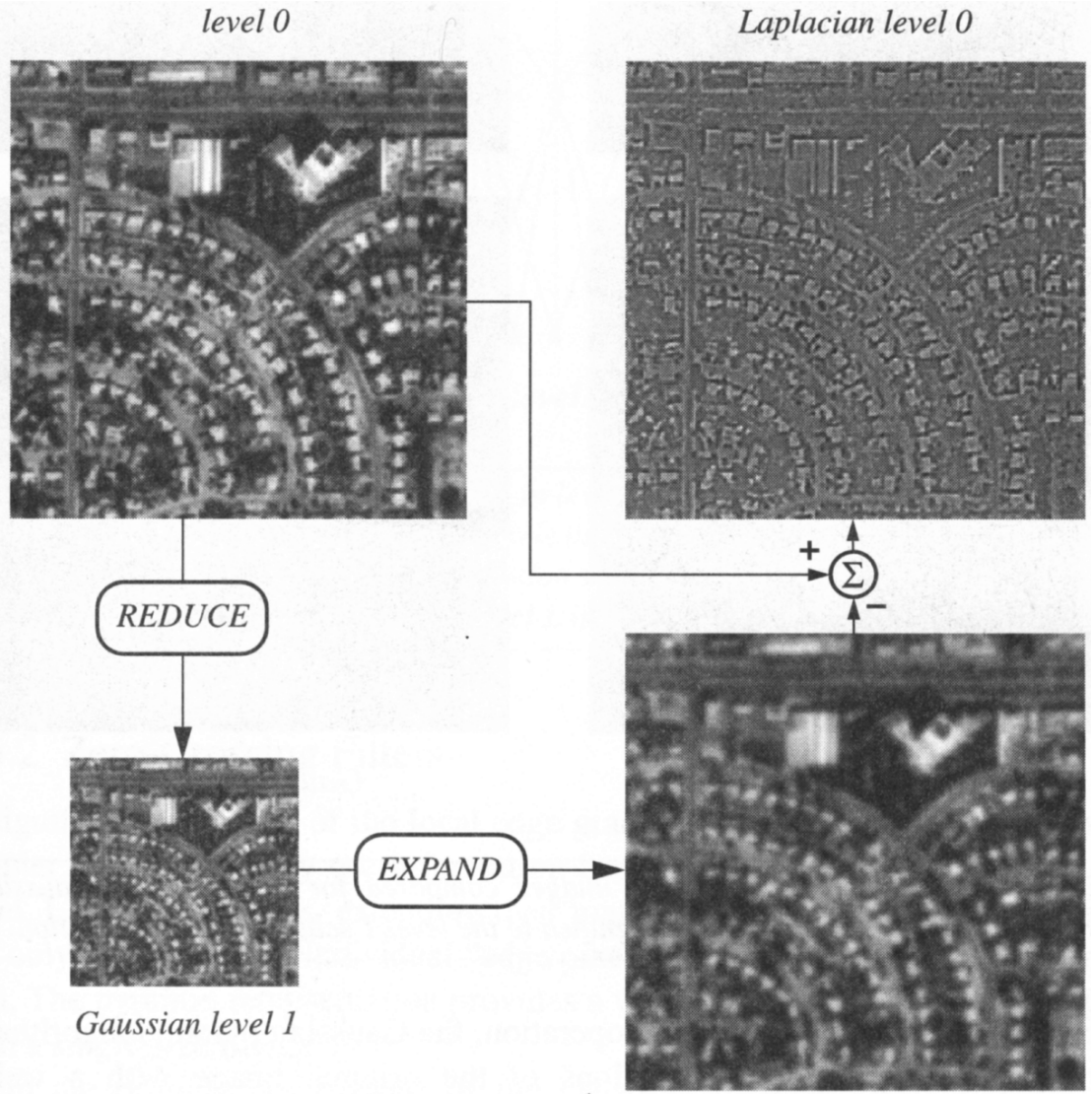

FIGURE 6-30. The construction of level 1 of the Gaussian pyramid and level 0 of the Laplacian pyramid. Level 2 would be constructed by the same process, starting at level 1. The Laplacian at level 1 would be calculated as the difference between the level 1 image and the EXPANDed Gaussian level 2 image.

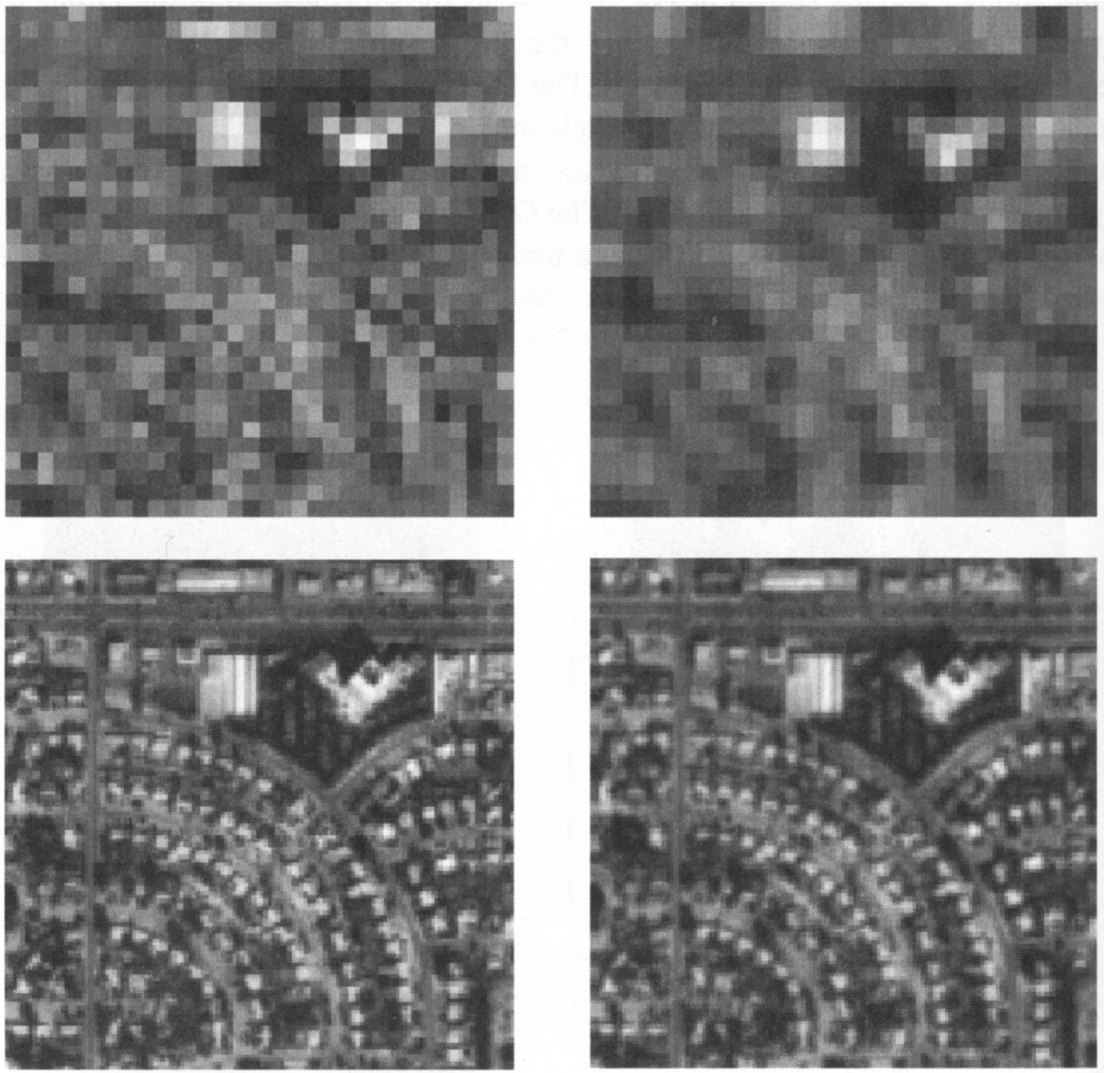

box pyramid *Gaussian pyramid*

FIGURE 6-31. Level 3 and level 1 images compared for the box and Gaussian pyramids. The level 3 images are magnified to the level 1 scale by pixel replication.

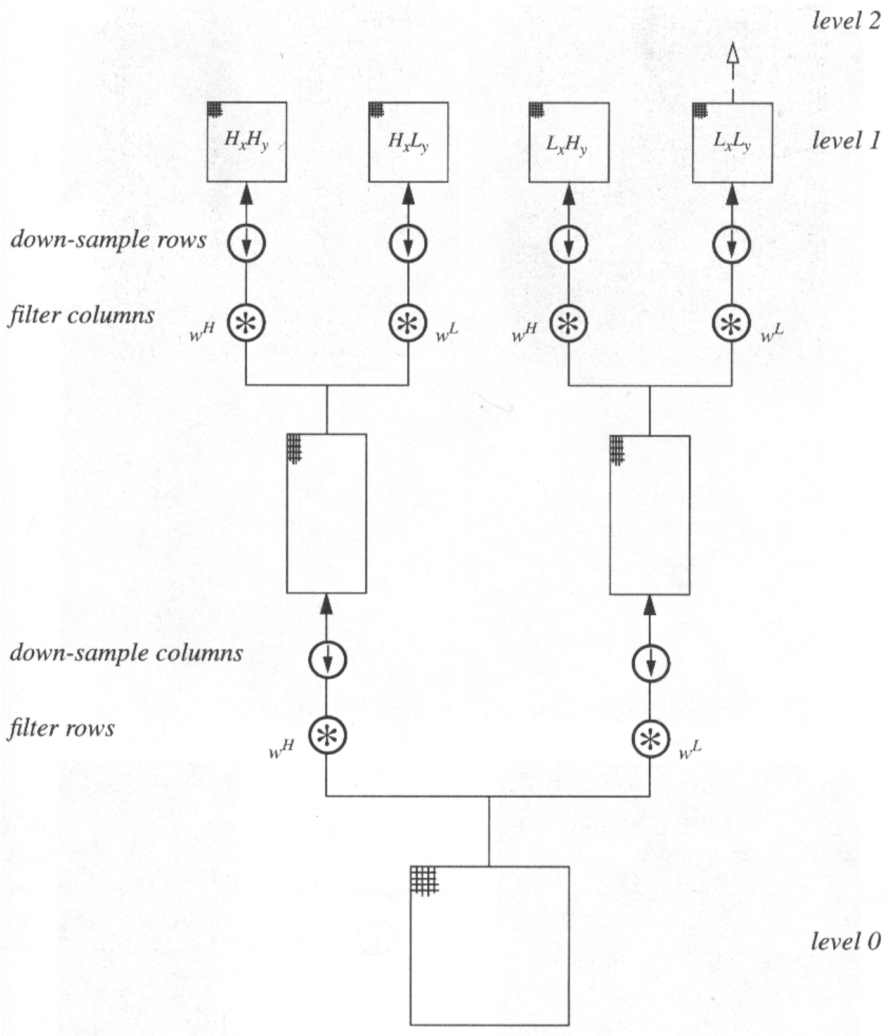

FIGURE 6-42. Wavelet decomposition from one pyramid level to the next. The letter L means low-pass and H means high-pass. Thus, L_xL_y means a low-pass filtered version that has been filtered in x (along rows) and y (along columns) and down-sampled by two. Likewise, H_xL_y means the image from the previous level is first high-pass filtered and down-sampled in x and then low-pass filtered and down-sampled in y. The L_xL_y component at each level is used as input to the calculations for the next level. This processing architecture is known as a filter bank.

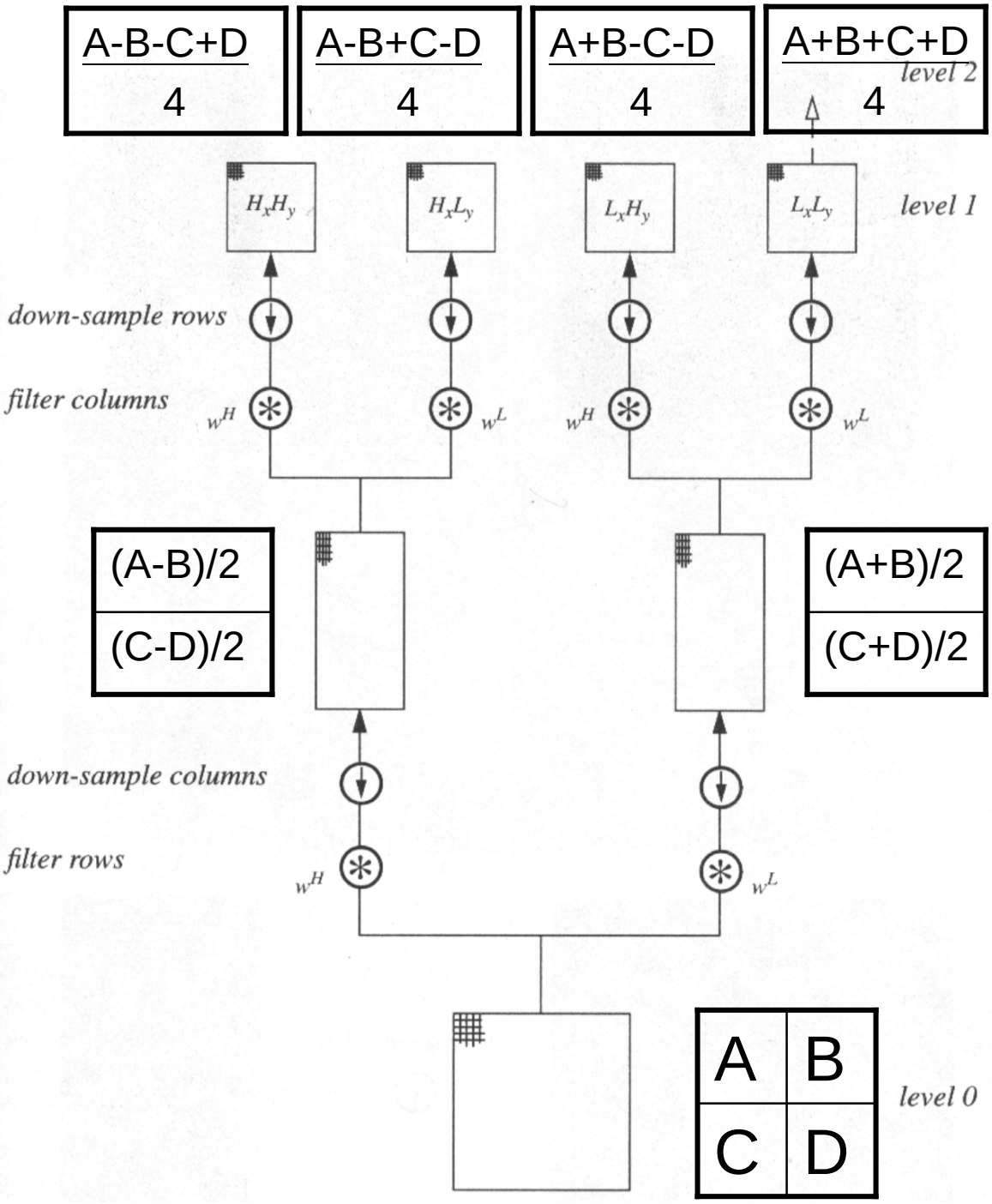

Haar Wavelet

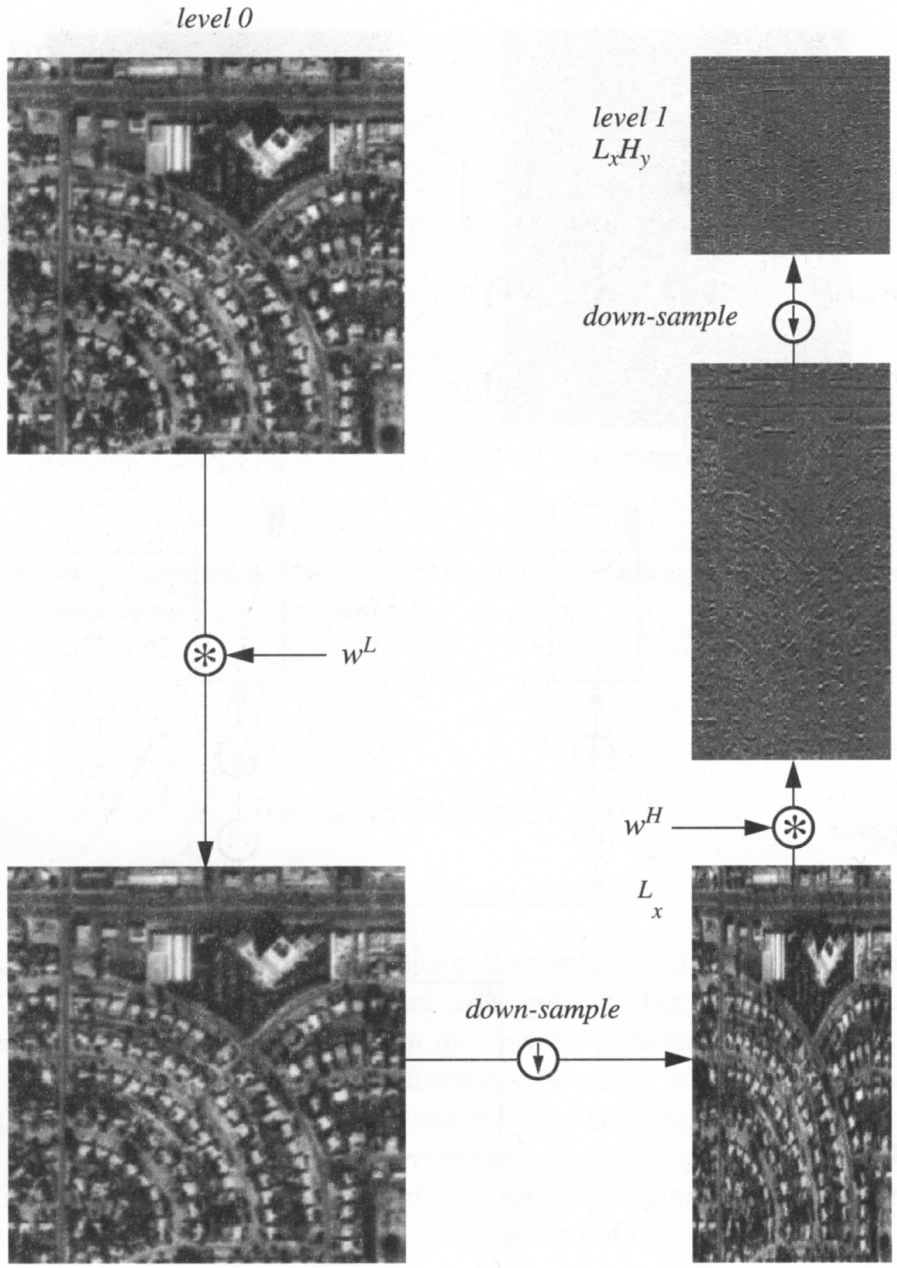

FIGURE 6-43. Calculation of one of the four wavelet components in level 1. The filtering and down-sampling combinations are similar to the REDUCE operation described earlier, except that here they are done one direction at a time.

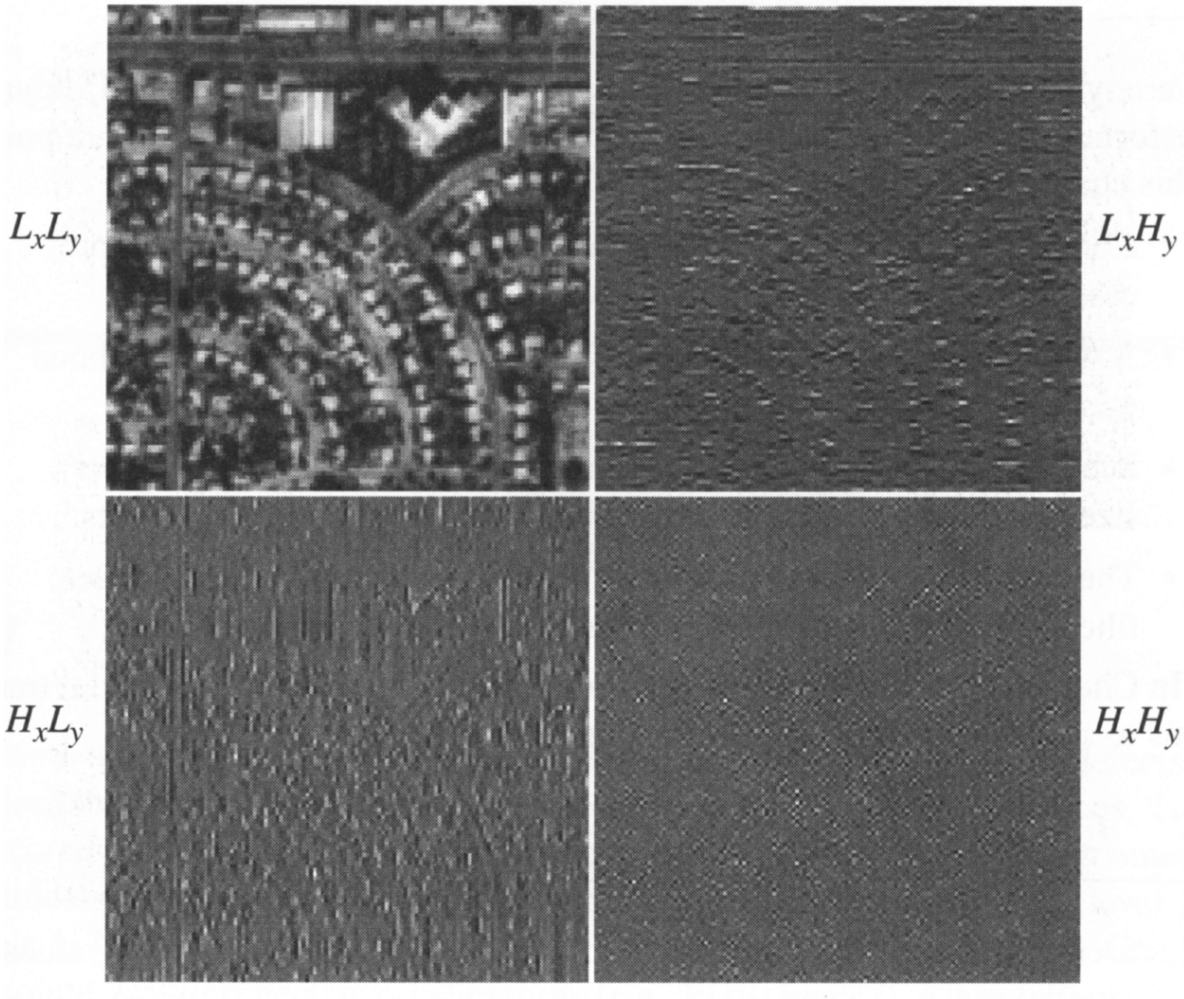

FIGURE 6-44. The four wavelet transform components of level 1 produced by the filter bank in Fig. 6-42. To create level 2, the upper left image, L_xL_y, is processed by the wavelet transform to produce a similar set of four images that are smaller by a factor of two in each direction.

Gaussian pyramid

```
dir *.lan
fid=fopen('paris.lan','r');
fseek(fid,128,-1)
A=fread(fid,[512*7,512],'uint8');
B=A(512*3+1:512*4,:);
Imagesc (B)
```

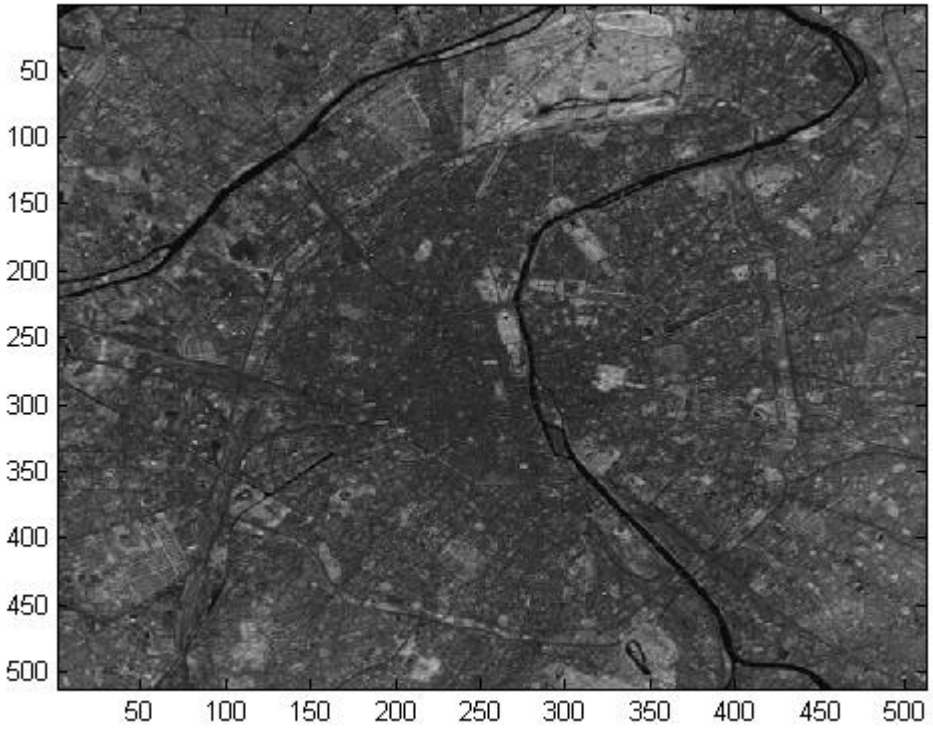

Gaussian pyramid

```
w=[0.05 0.25 0.4 0.25 0.05];
W=w'*w;
C=ones(size(B));
D=conv2(B,W,'same')./conv2(C,W,'same');
F=D(1:2:end,1:2:end);
```

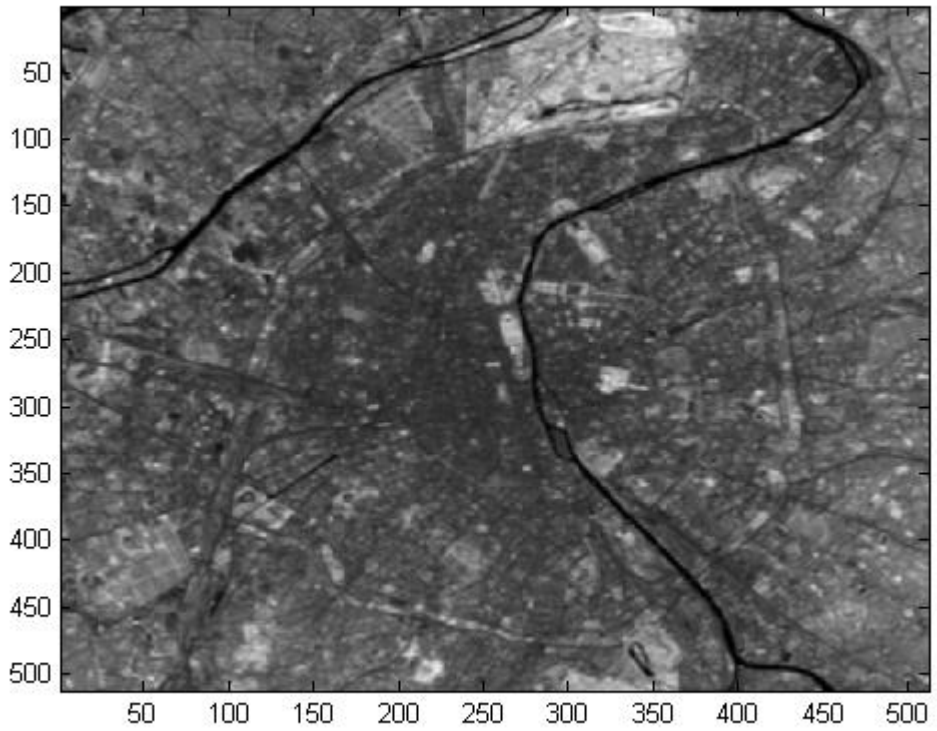

Gaussian expand

```
H=zeros(size(F)*2);
H(1:2:end,1:2:end)=F;
K=4*conv2(H,W,'same')./conv2(C,W,'same');
```

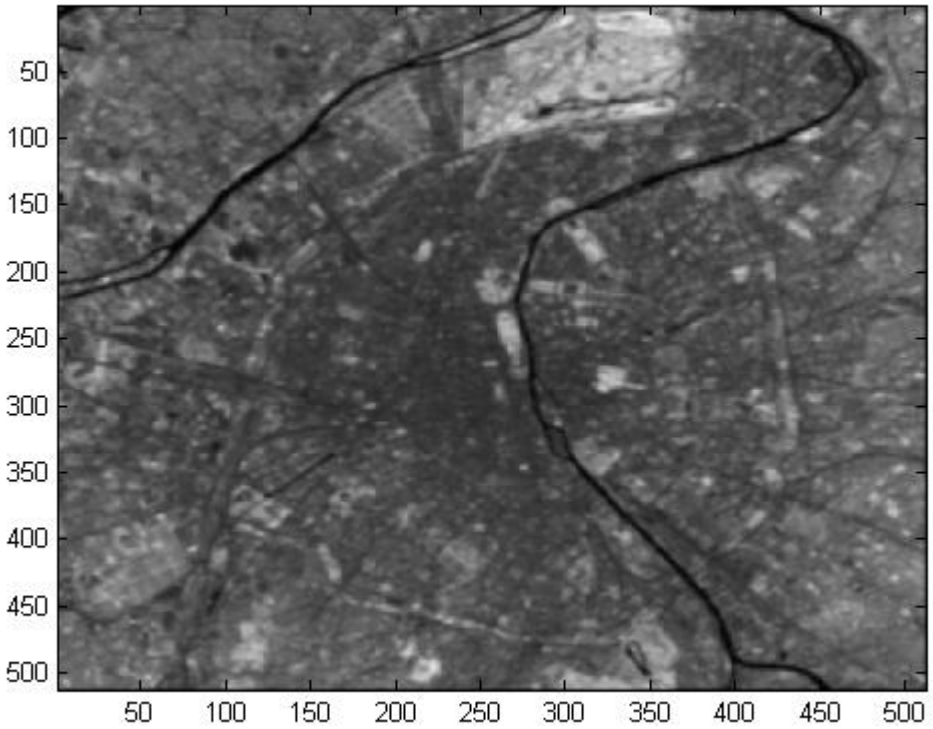

0.0025	0.0125	0.0200	0.0125	0.0025		
0.0125	0.0625	0.1000	0.0625	0.0125		
0.0200	0.1000	0.1600	0.1000	0.0200		
0.0125	0.0625	0.1000	0.0625	0.0125		
0.0025	0.0125	0.0200	0.0125	0.0025		

0.0025*4+0.02*4+0.16=0.25

0.0025	0.0125	0.0200	0.0125	0.0025		
0.0125	0.0625	0.1000	0.0625	0.0125		
0.0200	0.1000	0.1600	0.1000	0.0200		
0.0125	0.0625	0.1000	0.0625	0.0125		
0.0025	0.0125	0.0200	0.0125	0.0025		

0.0125*4+0.1*2=0.25

	0.0025	0.0125	0.0200	0.0125	0.0025	
	0.0125	0.0625	0.1000	0.0625	0.0125	
	0.0200	0.1000	0.1600	0.1000	0.0200	
	0.0125	0.0625	0.1000	0.0625	0.0125	
	0.0025	0.0125	0.0200	0.0125	0.0025	

0.0625*4=0.25

Laplacian pyramid

L=B-K;

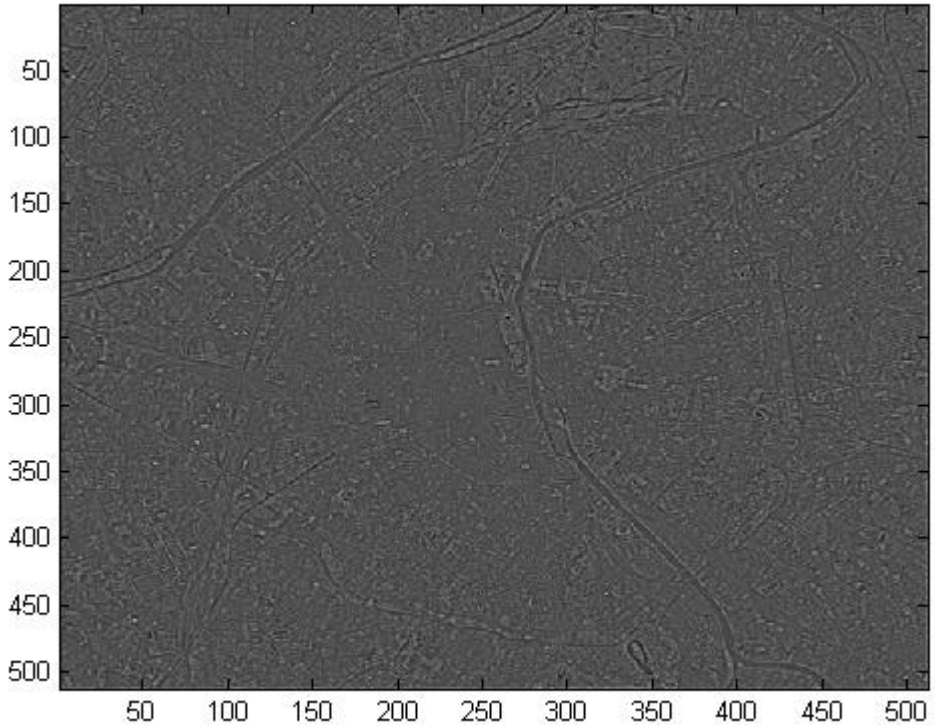

PCT

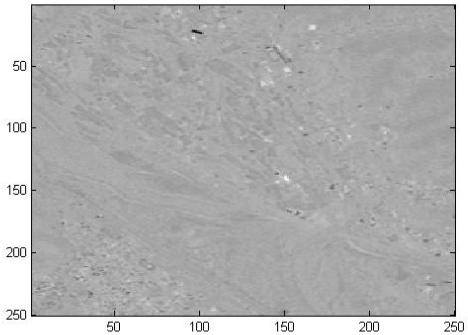

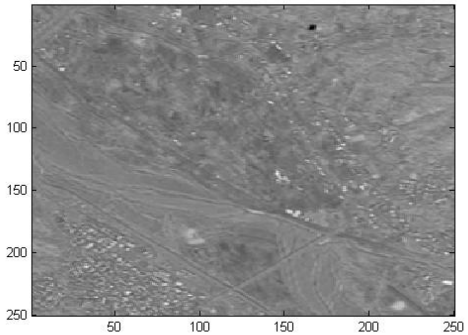

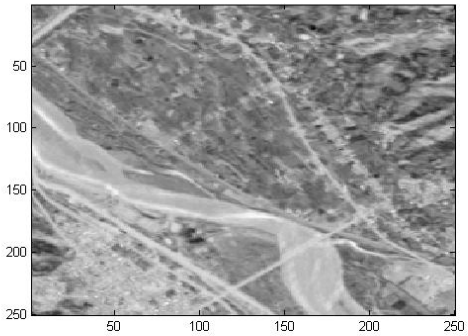

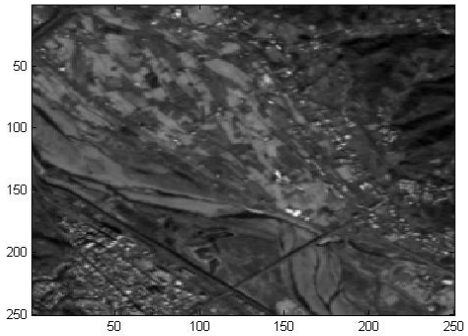


```
z=reshape(A1,250*250,4)';
mu=mean(z')';
C=double(z)*double(z)'/(250*250)-mu*mu';
[V,D]=eig(C);
Z1=V'*double(z);
Z1=reshape(Z1',250,250,4);
for i=1:4
    subplot(2,2,i)
    imagesc(Z1(:,:,i))
end
colormap(gray)
```

PCT

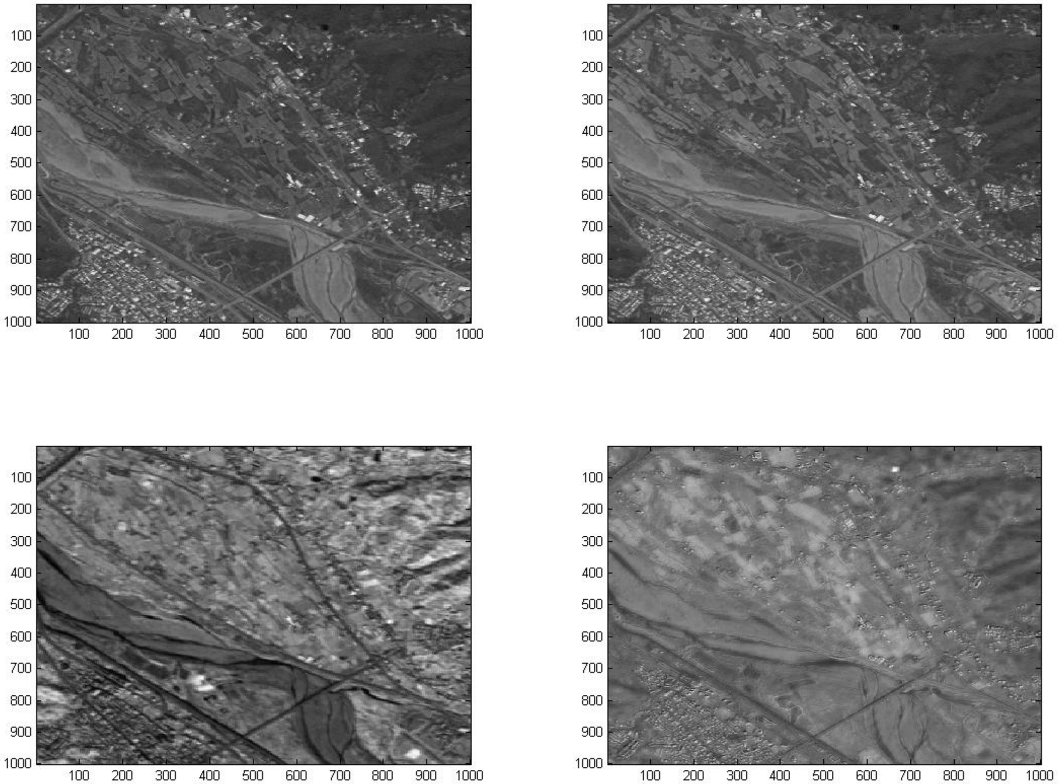

```
F=zeros(1000,1000,4);
for i=1:4,for j=1:4
        F(i:4:end,j:4:end,:)=Z1;
    end,end
A=double(A);
B=(A-min(min(A)))/(max(max(A))…
                    -min(min(A)))*(m1-m2)+m2;
F(:,:,4)=A;
G=V*reshape(F,1000*1000,4)';
G=reshape(G',1000,1000,4)
for i=1:4
    subplot(2,2,i)
    imagesc(G(:,:,i))
end
```

Color Space Transform

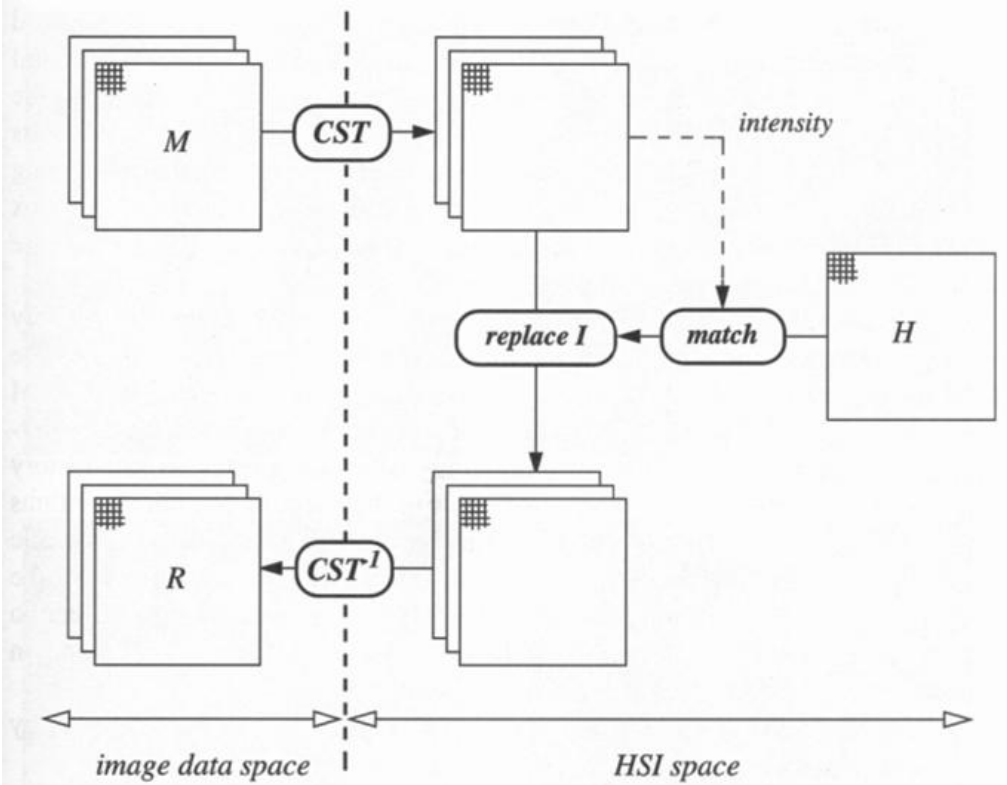

FIGURE 8-14. Image fusion using a color space transform (CST) and replacement of the intensity component. The multispectral image M has been previously registered to the high resolution image H.

CST

```
load fusion_spot
imagesc(A)
colormap(gray)
figure
image(A1(:,:,[3 2 1]))
```

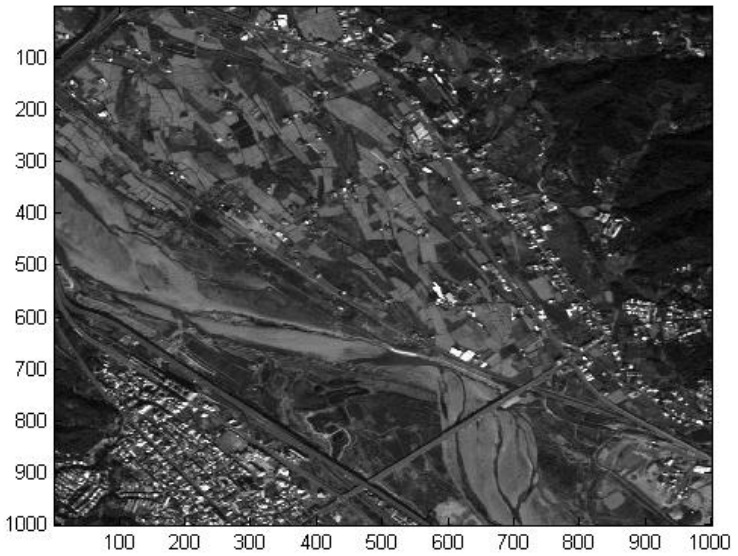

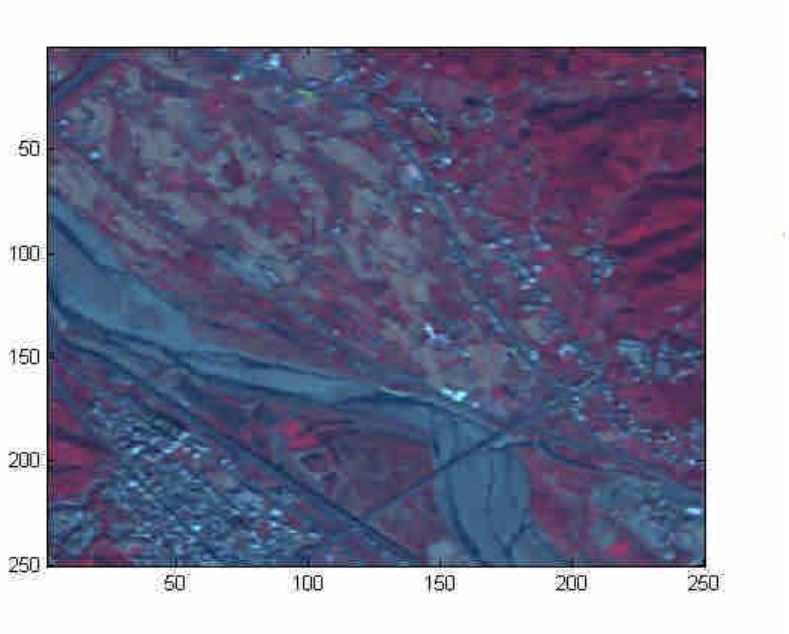

CST

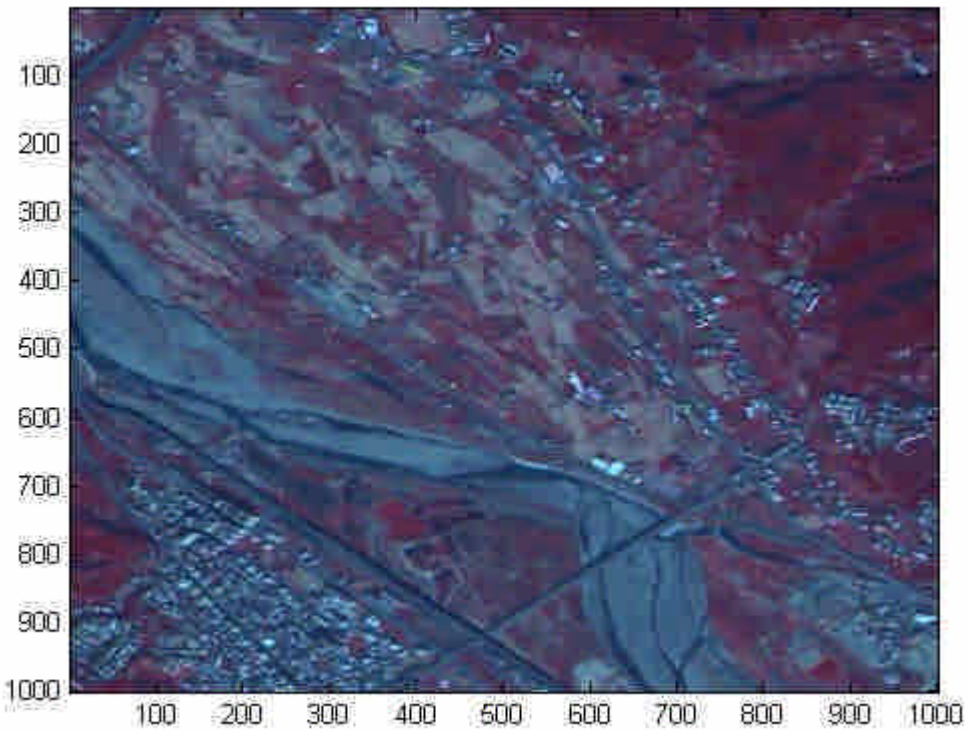


```
C=rgb2hsv(B);
D=zeros(1000,1000,3);
for i=1:4,for j=1:4
    D(i:4:end,j:4:end,:)=C;
end,end
D(:,:,3)=double(A)/255;
F=hsv2rgb(D);
```

光譜解析度

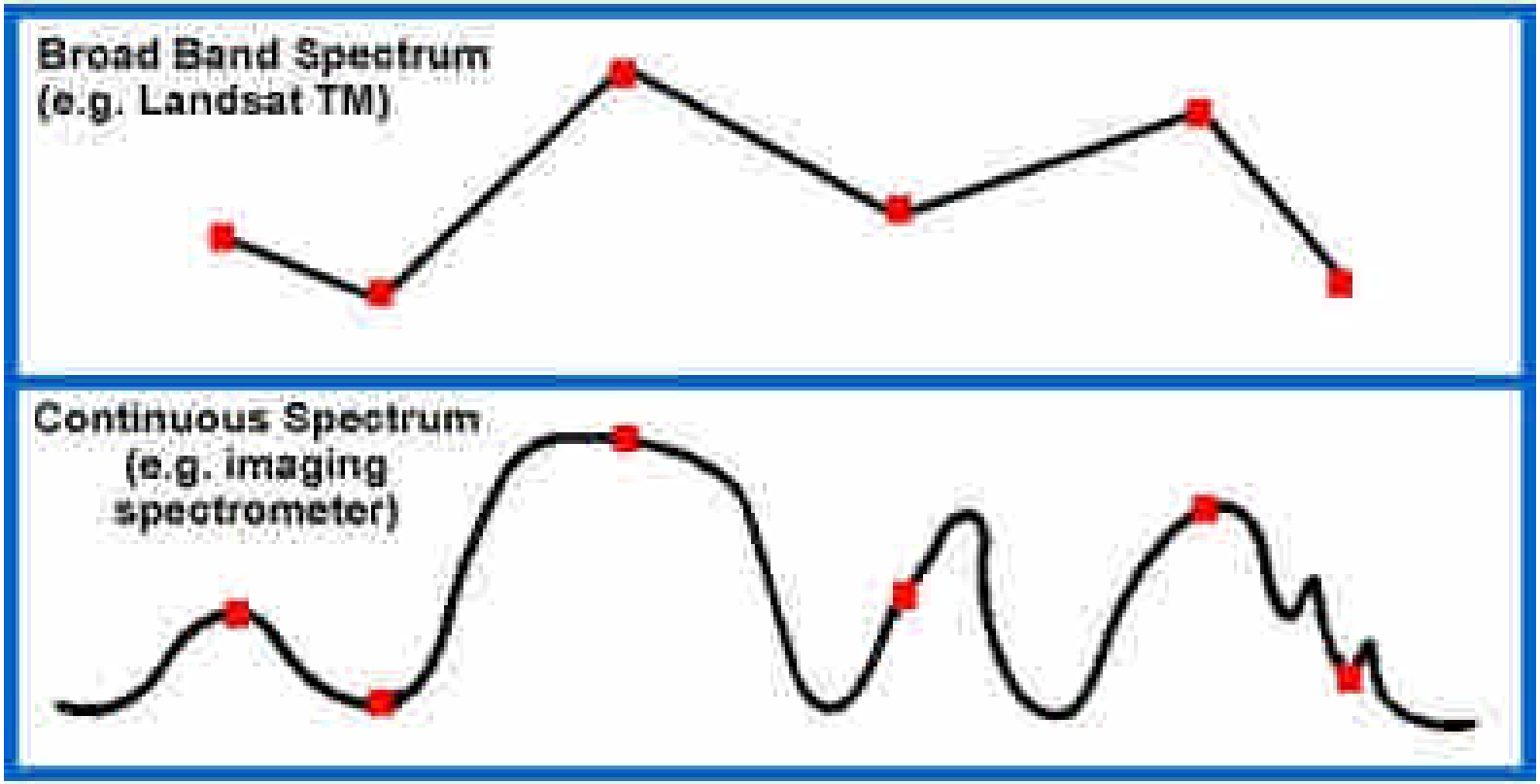
Broad Band Spectrum
(e.g. Landsat TM)
Continuous Spectrum
(e.g. imaging
spectrometer)

- 多光譜與高光譜

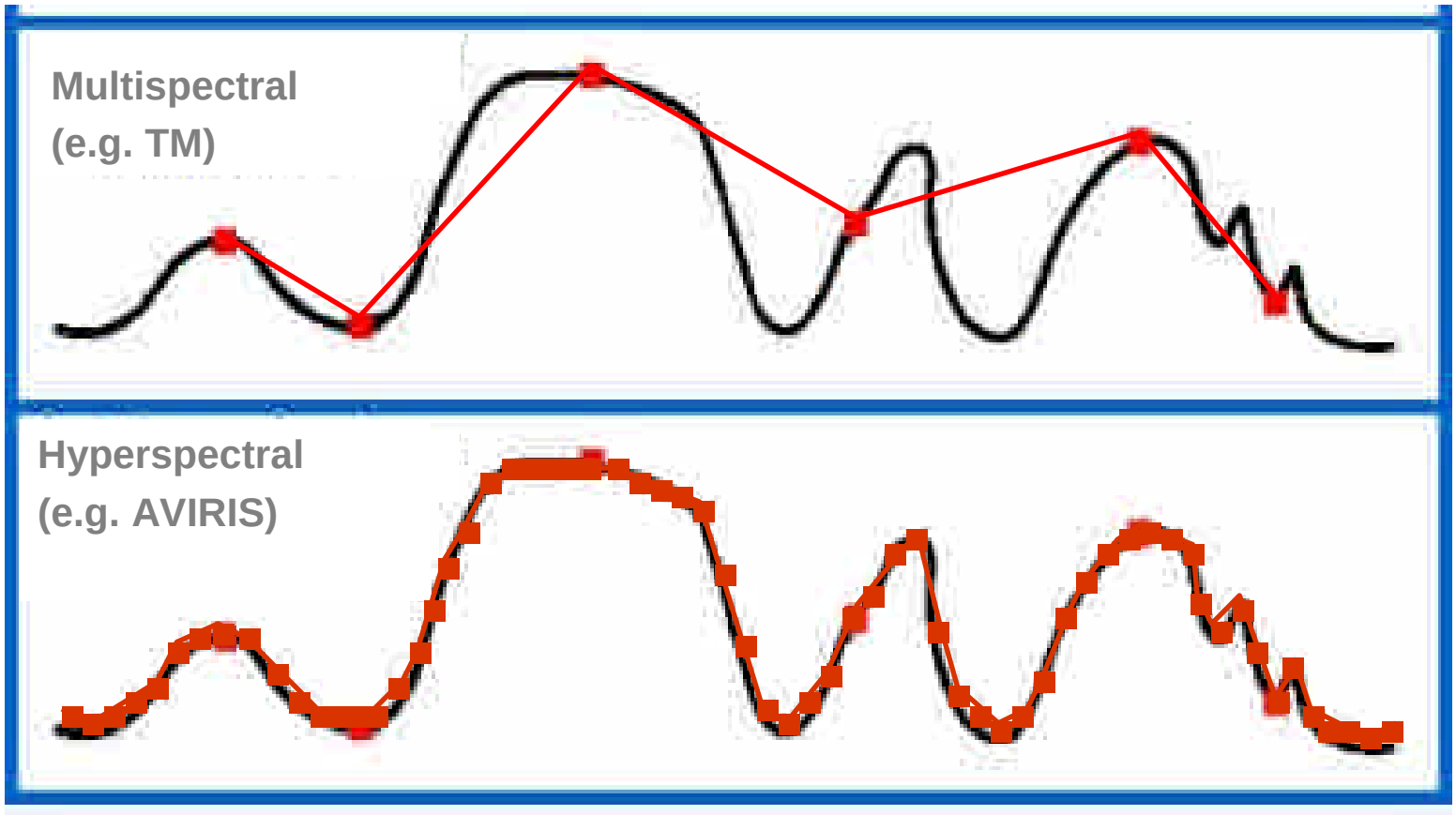

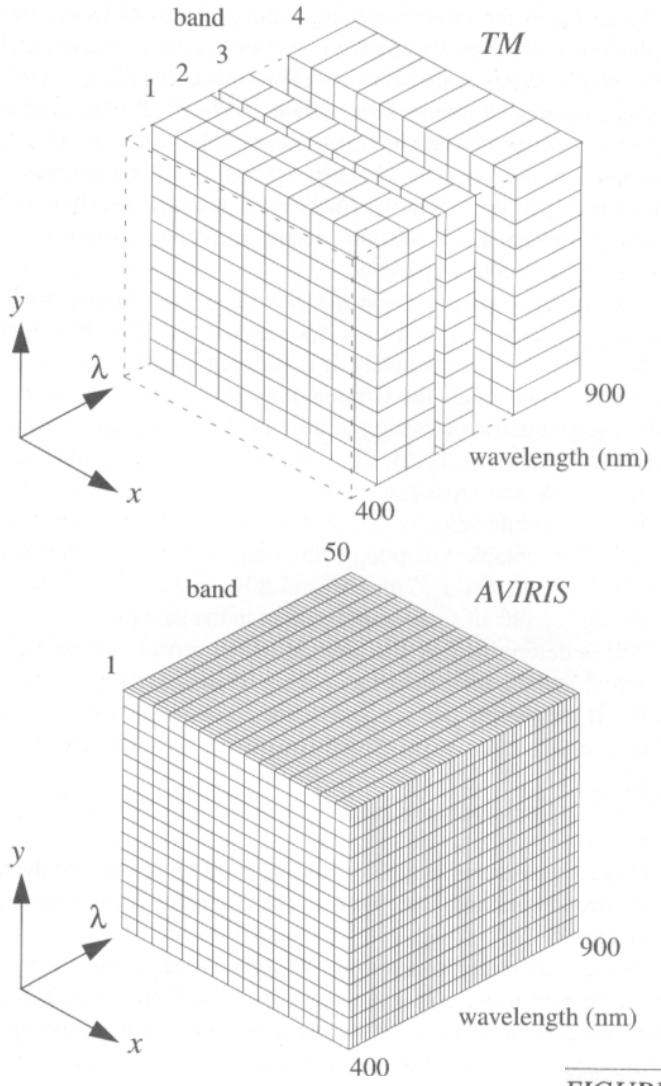

FIGURE 1-7. Visualization of the spatial and spectral resolutions of the Landsat TM and AVIRIS in the VNIR spectral range. The relative proportions between the two sensors are correct along each axis, and each small rectangular box represents one image pixel. The TM samples the spectral dimension incompletely and with relatively broad spectral bands. In comparison, AVIRIS represents almost a continuous spectral sampling. It also has a somewhat smaller GIFOV. This volume visualization is called an "image cube."

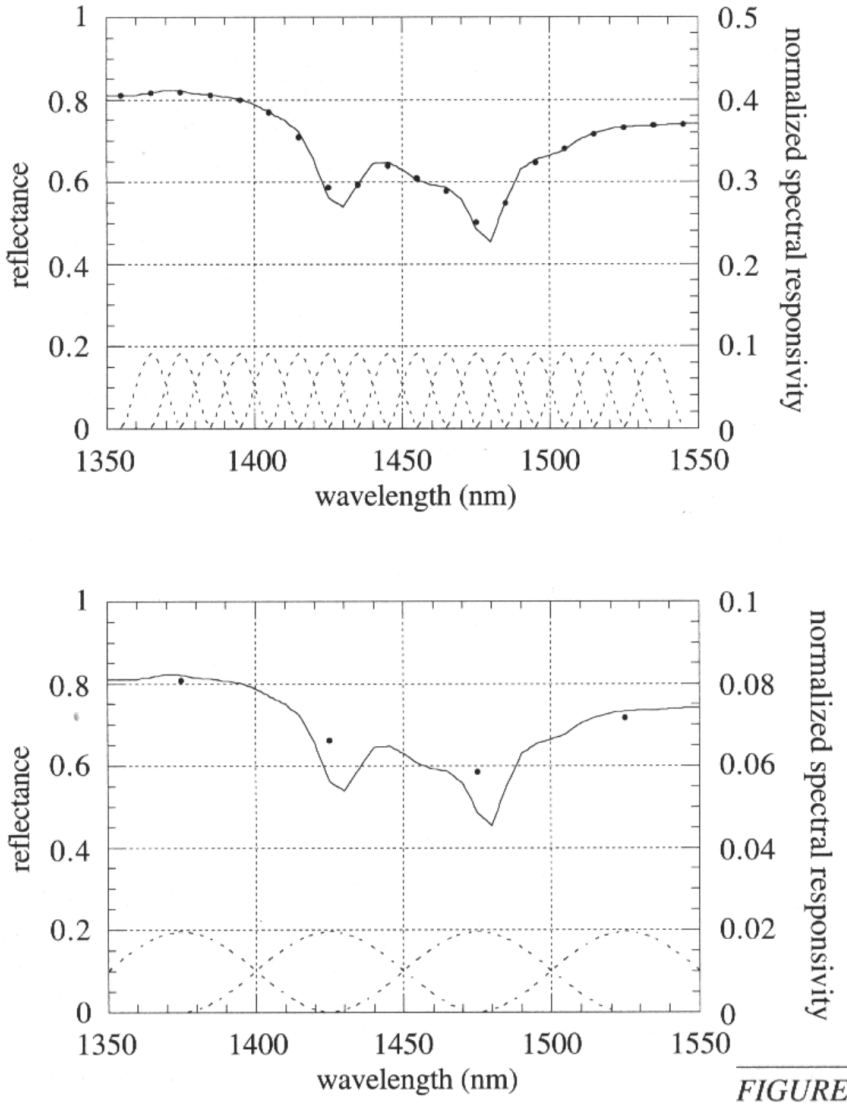

FIGURE 3-6. The effective reflectance of alunite as measured by a multispectral sensor. The solid line is the original reflectance sampled at 1nm and the individual band spectral responsivities are shown as dashed lines. Each solid dot is the output of the corresponding band. The upper graph corresponds to a sensor with 10nm-wide spectral bands, which approximates a hyperspectral sensor such as AVIRIS or HYDICE. The lower graph represents a sensor with 50nm-wide spectral bands, such as TM (although TM does not actually have any spectral bands in this part of the spectrum).

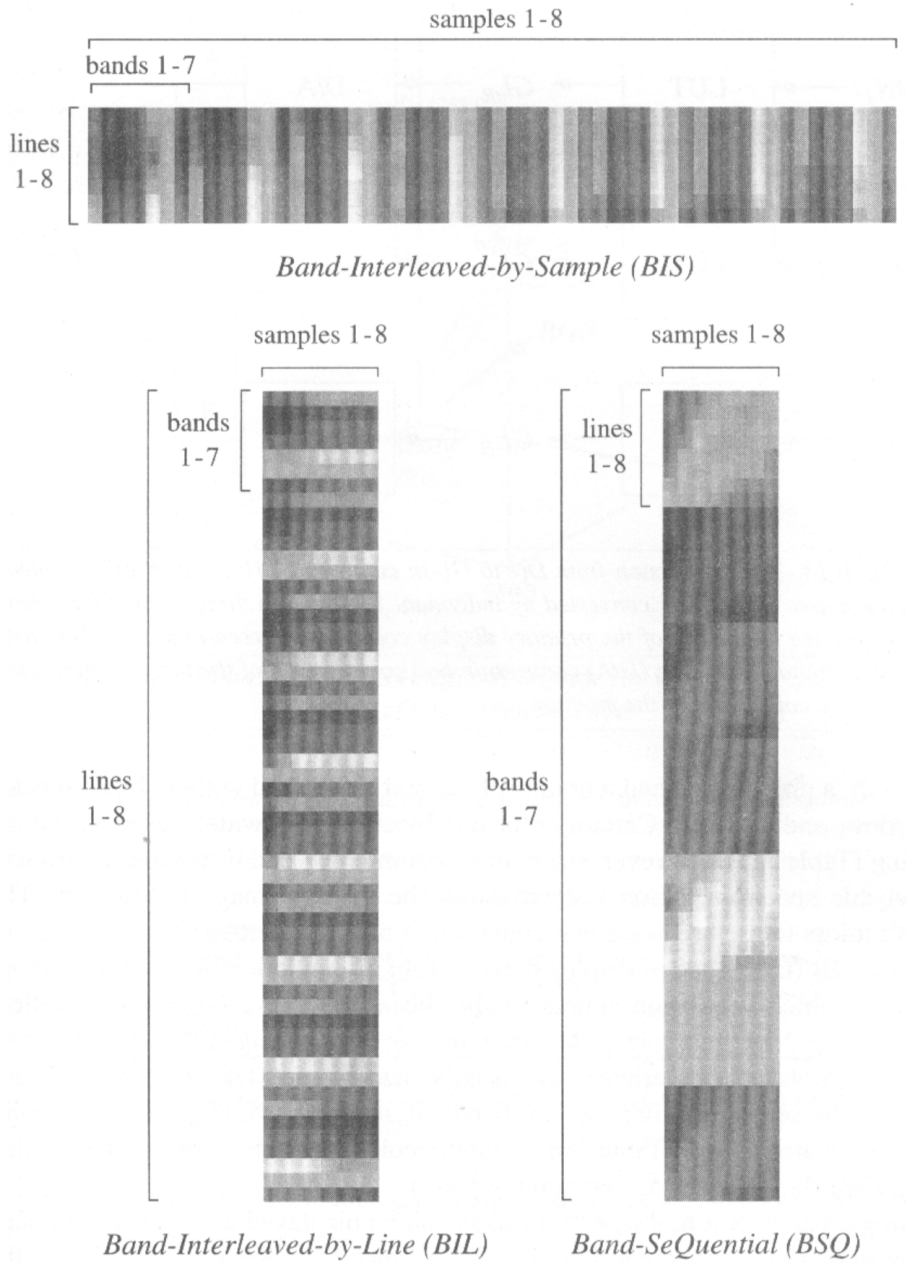

FIGURE 1-12. The three most common multispectral image formats: BIS, BIL and BSQ, illustrated with an 8 sample-by-8 line-by-7 band TM image. Note the very low contrast in the TIR band 6 relative to the other bands.

- 光譜解析度

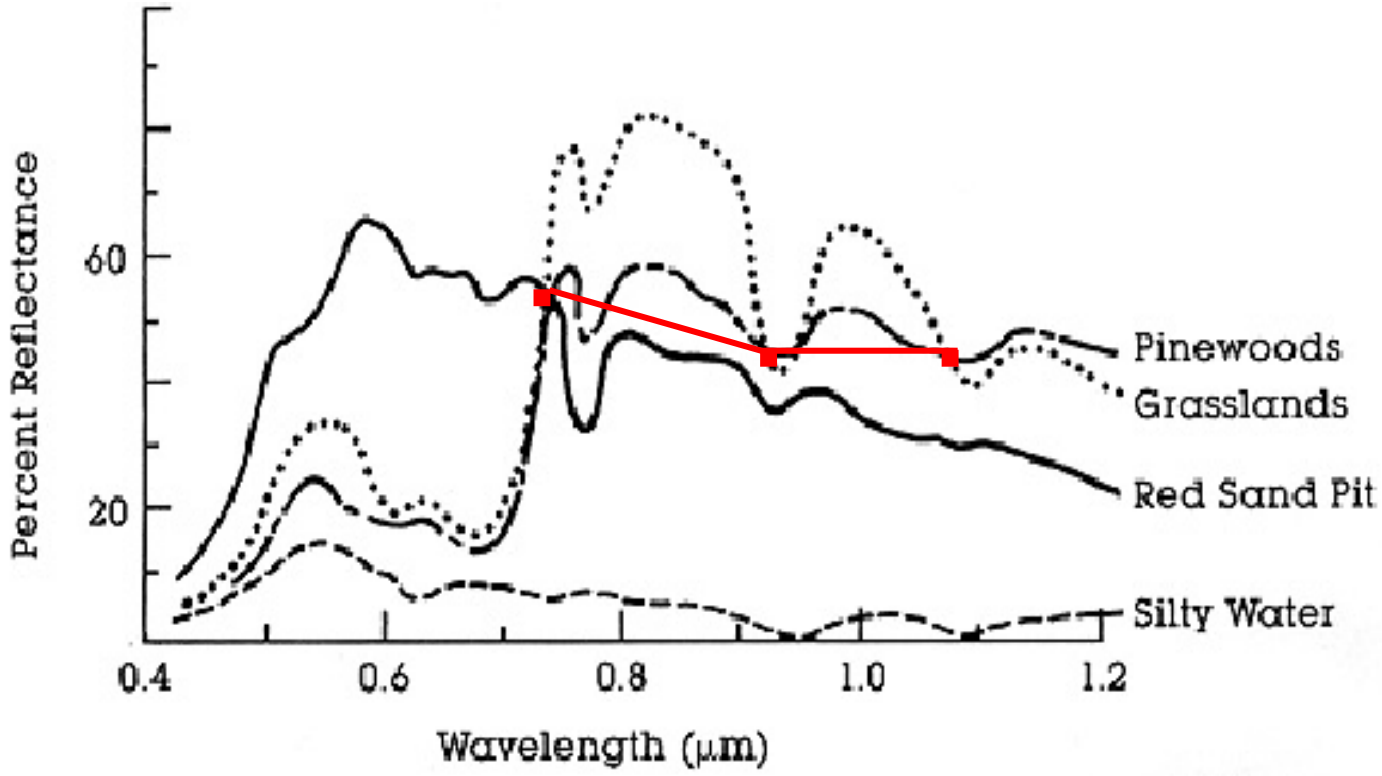
Percent Reflectance
60
20
0.4
0.6
0.8
1.0
1.2
Wavelength (μm)
Pinewoods
Grasslands
Red Sand Pit
Silty Water

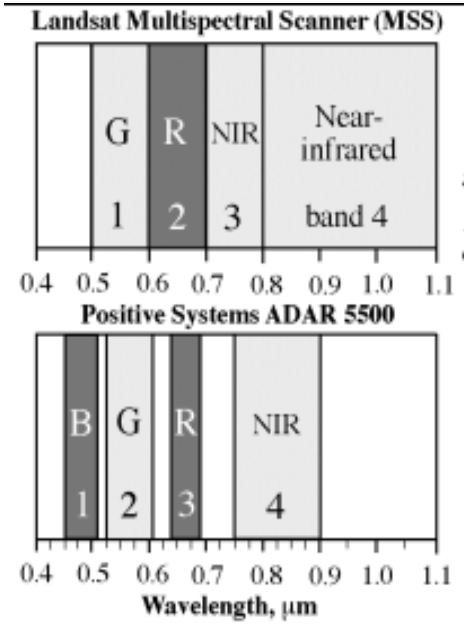

a. Nominal spectral resolution of the Landsat Multispectral Scanner and Positive Systems ADAR 5500 digital frame camera.

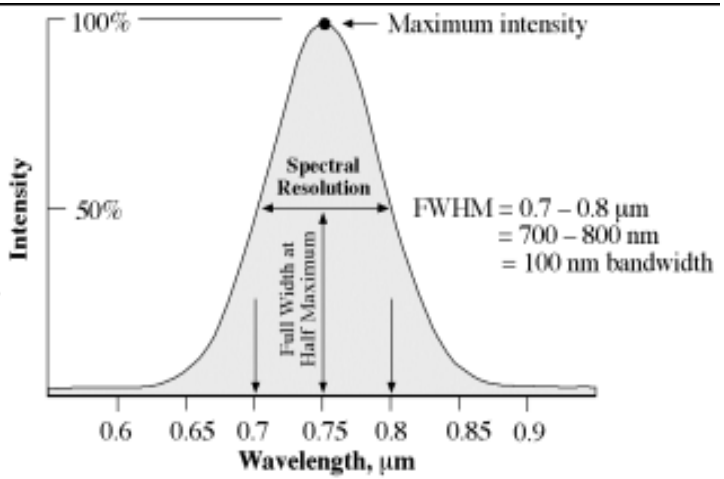

b. Precise bandpass measurement of a detector based on Full Width at Half Maximum (FWHM) criteria

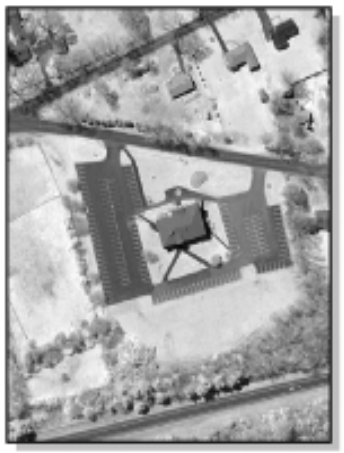

c. Single band of ADAR 5500 data

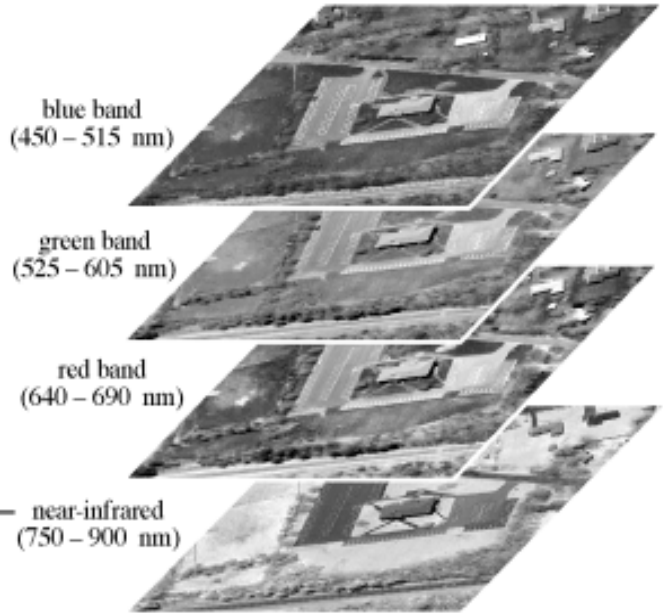

d. Multispectral remote sensing

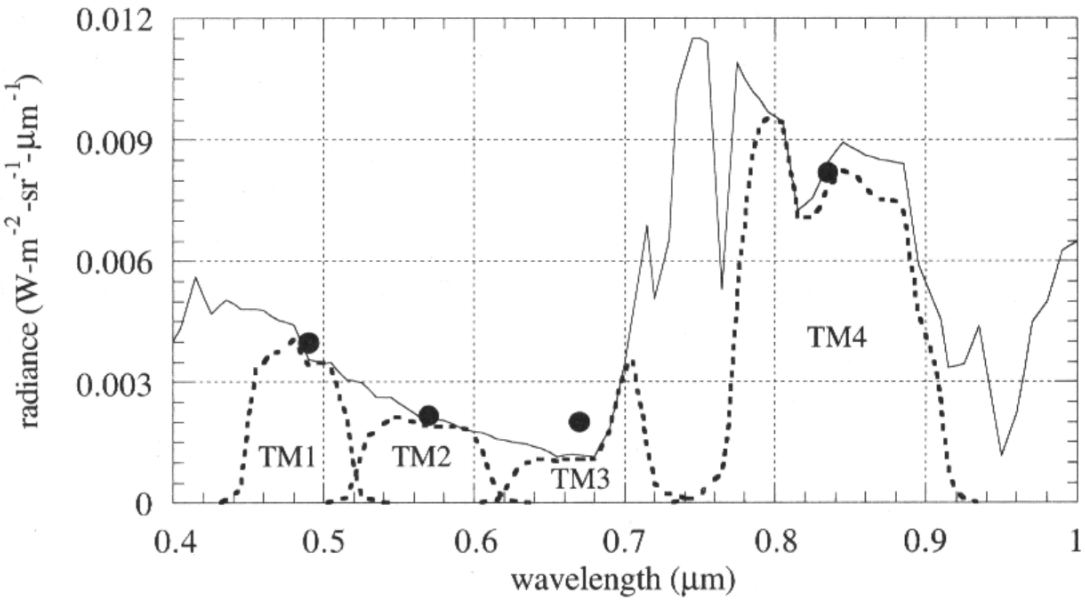

FIGURE 3-7. The at-sensor radiance for Kentucky Bluegrass (solid curve), the weighted spectral distribution seen by each TM band (dotted curves), and the total (integrated over the weighted spectral distribution) effective radiance (solid circles). Note how the broad bandwidth of bands 3 and 4, in particular, averages spectral detail present in the original radiance.

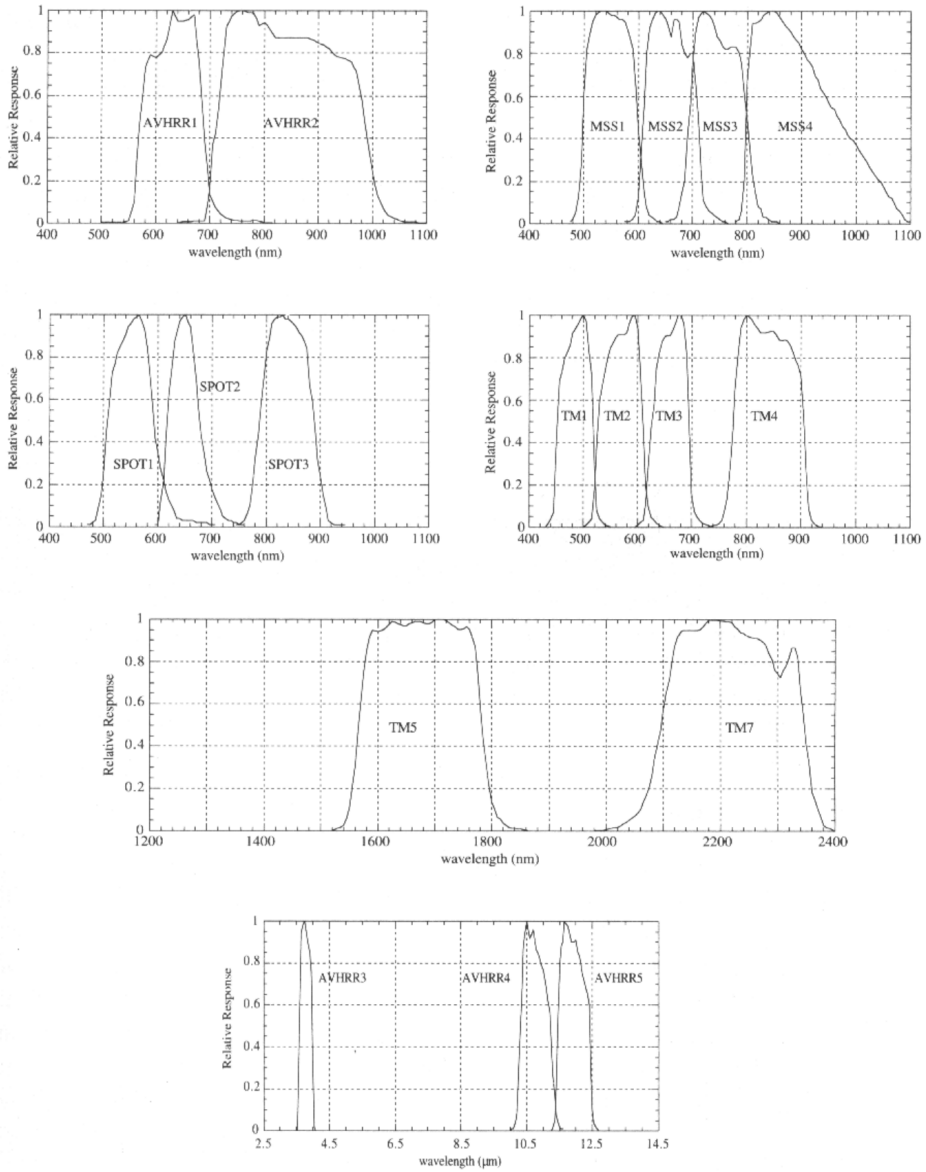

FIGURE 3-8. Normalized spectral response functions for the AVHRR, MSS, SPOT, and TM sensors. These data are only meant to be representative; individual detectors within a band can vary by several percent. Note the passbands are not rectangular and neighboring bands often overlap. An absolute vertical scale is determined by the responsivity of the detectors measured in electron units, e.g. amps or volts per unit irradiance.

灰階解析度

時間解析度

系統	時間解析度(天)
Landsat 1, 2, 3	18
Landsat 4, 5	16
AVHRR	1
SPOT	26
MODIS	2

sensor	axis name	W_{TC}
	MSS band	1 2 3 4
L-1 MSS	soil brightness	+0.433 +0.632 +0.586 +0.264
	greenness	–0.290 –0.562 +0.600 +0.491
	yellow stuff	–0.829 +0.522 –0.039 +0.194
	non-such	+0.223 +0.120 –0.543 +0.810
L-2 MSS	soil brightness	+0.332 +0.603 +0.676 +0.263
	greenness	+0.283 –0.660 +0.577 +0.388
	yellow stuff	+0.900 +0.428 +0.0759 –0.041
	non-such	+0.016 +0.428 –0.452 +0.882
	TM band	1 2 3 4 5 7
L-4 TM	soil brightness	+0.3037 +0.2793 +0.4743 +0.5585 +0.5082 +0.1863
	greenness	–0.2848 –0.2435 –0.5436 +0.7243 +0.0840 –0.1800
	wetness	+0.1509 +0.1973 +0.3279 +0.3406 –0.7112 –0.4572
	haze	–0.8242 +0.0849 +0.4392 –0.0580 +0.2012 –0.2768
	TC5	–0.3280 +0.0549 +0.1075 +0.1855 –0.4357 +0.8085
	TC6	+0.1084 –0.9022 +0.4120 +0.0573 –0.0251 +0.0238
L-5 TM	soil brightness	+0.2909 +0.2493 +0.4806 +0.5568 +0.4438 +0.1706
	greenness	–0.2728 –0.2174 –0.5508 +0.7221 +0.0733 –0.1648
	wetness	+0.1446 +0.1761 +0.3322 +0.3396 –0.6210 –0.4186
	haze	+0.8461 +0.0731 +0.4640 –0.0032 –0.0492 +0.0119
	TC5	+0.0549 –0.0232 +0.0339 –0.1937 +0.4162 –0.7823
	TC6	+0.1186 –0.8069 +0.4094 +0.0571 –0.0228 +0.0220
	soil brightness	additive terms: +10.3695
	greenness	–0.7310
	wetness	–3.3828
	haze	+0.7879
	TC5	–2.4750
	TC6	–0.0336

TABLE 5-2. Tasseled-cap coefficients for Landsat-1 MSS (Kauth and Thomas, 1976), Landsat-2 MSS (Thompson and Whemanen, 1980), Landsat-4 TM (Crist and Cicone, 1984) and Landsat-5 TM (Crist et al., 1986). The MSS coefficients are for a 0-63 DN scale in band 4 and a 0-127 DN scale in the other bands, i.e. the same as data supplied to users.

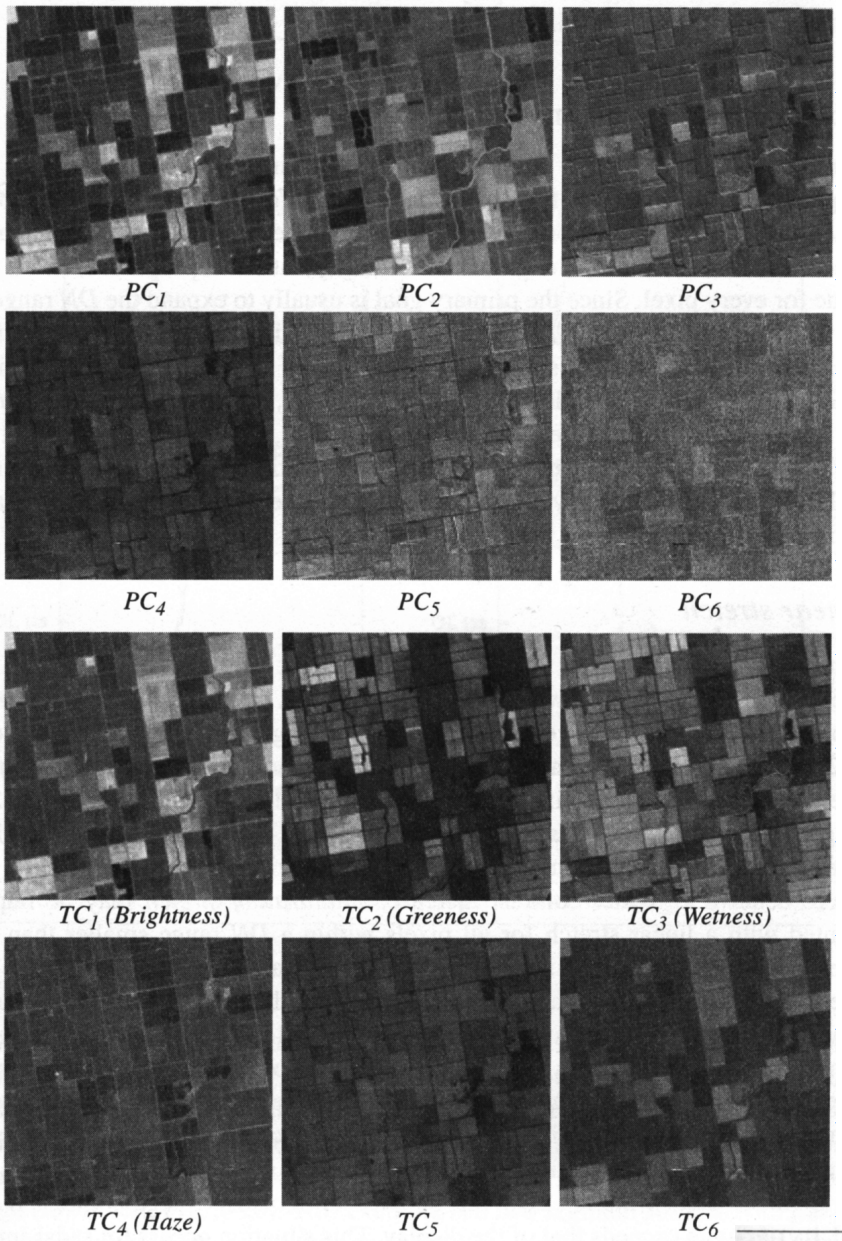

FIGURE 5-18. The PC and TC components for the Yuma agricultural scene. The PCT achieves more data compression (PC_5 and PC_6 contain almost no scene content), but the TCT better represents soil and vegetation in TC_1 and TC_2. Note PC_2 is inverted relative to TC_2.

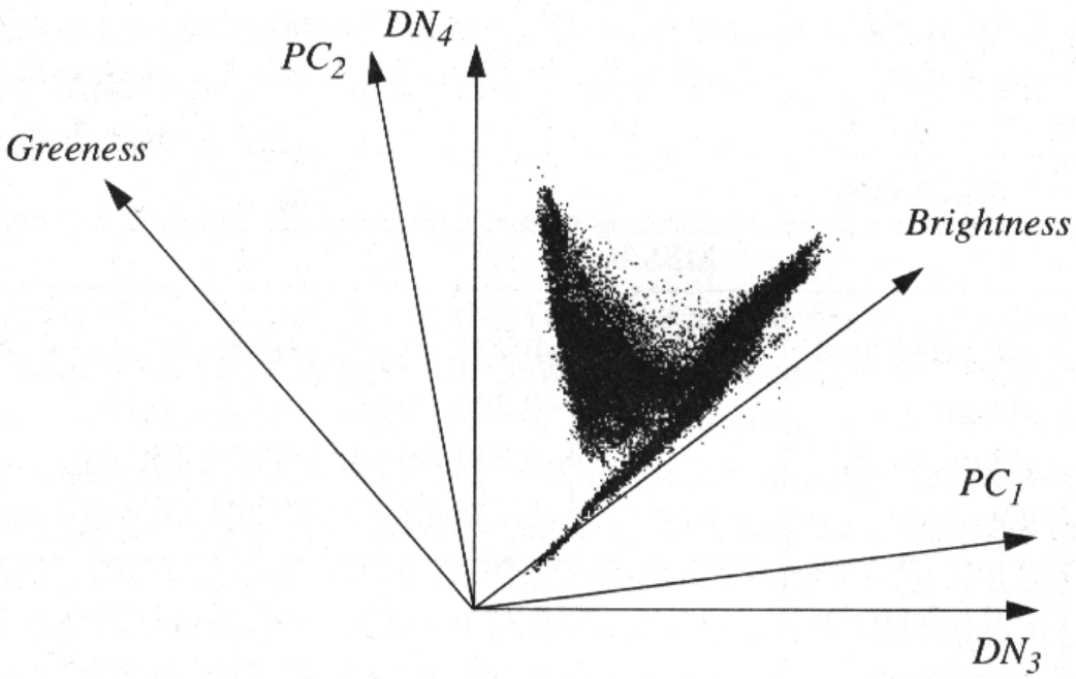

FIGURE 5-17. Projection of two of the component axes from 6-D PC and TC transformations onto the TM band 4 versus band 3 data plane. The Brightness-Greenness projection is fixed and independent of the data. Notice how the Brightness-Greenness space "captures" the physical components of soil and vegetation better than does the PC_1-PC_2 space.